

# Role of reptation in the rate of crystallization of polyethylene fractions from the melt

John D. Hoffman

National Bureau of Standards, Washington, DC 20234, USA

(Received 19 October 1981)

The theory of polymer crystallization with chain folding is extended to include the effect of reptation in the melt on the rates of crystallization  $G_I$  and  $G_{II}$  in régimes I and II. The result is that the pre-exponential factors for  $G_I$  and  $G_{II}$  contain a factor  $1/n$ , where  $n$  is the number of monomer units in the pendant chain being reeled onto the substrate by the force of crystallization;  $n$  is proportional to the molecular weight. The predicted fall in growth rate with increasing molecular weight is found experimentally in nine polyethylene fractions  $M_z=2.65 \times 10^4$  to  $M_z=2.04 \times 10^5$ , corresponding to  $n_z=1.90 \times 10^3$  to  $1.45 \times 10^4$ . The data on these fractions are analysed to find the reptation or 'reeling' rate  $r$  and the substrate completion rate  $g$ . The values  $g_{nuc} \sim 0.5/n_z \text{ cm s}^{-1}$  and  $r_{nuc} \sim 21/n_z \text{ cm s}^{-1}$  at 400K are obtained from the data in conjunction with nucleation theory adapted to account for reptation assuming a substantial degree of regular folding. These results are consistent with a melting point in the range of  $\sim 142^\circ$  to  $\sim 145^\circ\text{C}$ . (The analysis using  $T_m(\infty) = 145^\circ\text{C}$  gives values of such quantities as  $\sigma\sigma_e$  and  $\alpha$  that are quite similar to those deduced in earlier studies.) An estimate of  $g$  (denoted  $g_{expt}$ ) that is independent of the molecular details of nucleation theory gives  $g_{expt} \sim 0.4/n_z \text{ cm s}^{-1}$  and  $r \sim 17/n_z \text{ cm s}^{-1}$  at 400K. Calculations of the reptation rate from  $r_{1,2} = (\text{force of crystallization} \div \text{friction coefficient for reptation in melt})$ , where the friction coefficient is determined from diffusion data on polyethylene melts, leads to  $r_{1,2} \sim 17/n_z$  to  $34/n_z \text{ cm s}^{-1}$  at 400K, or  $g_{1,2} \sim 0.4/n_z$  to  $0.8/n_z \text{ cm s}^{-1}$ . The conclusion is that the reptation rate characteristic of the melt is fast enough to allow a significant degree of adjacent re-entry or 'regular' folding during substrate completion at the temperature cited, and that the substrate completion process is governed jointly by the activation energy for reptation  $Q_D^*$  and the work of chain folding  $q$ . The nucleation theory and the friction coefficient theory approaches are compared, and the formulations found to be essentially equivalent; the 'reeling' rate  $r$  is found to be proportional to  $(1/n)A_0(\Delta f)v_0 \exp[-(Q_D^* + q)/RT]$ , where  $v_0$  is a frequency factor, and  $A_0(\Delta f)$  is the force of crystallization on the pendant chain. The data analysis on the fractions confirms the detailed applicability of régime theory. The growth rate theory presented allows the possibility that the growth front may be microfaceted in régime I.

**Keywords** Crystallization; polyethylene; reptation; growth rate; fraction; friction coefficient; régime I; régime II

## INTRODUCTION

The kinetic nucleation theory with chain-folding provides the best overall theoretical framework now available for understanding the rate of isothermal crystallization of linear polymers from the unstrained melt and from dilute solution<sup>1</sup>. This theory provides a rationale not only for the rate of crystallization itself but also for the chain-folding that occurs, the lamellar or plate-like structures that are commonly observed, and the variation of the initial thickness of these structures with crystallization temperature<sup>1,2</sup>. The simple form of the theory treats the limiting case of fully-adjacent re-entry. However, this creates little general difficulty in estimating the lamellar thickness and growth rate, since, under many conditions, considerations of topological origin based on the necessity of avoiding a density anomaly at the liquid-crystal interface demand a rather high degree of adjacent re-entry or tight folding<sup>3,4</sup>. Here, we shall treat the effect of reptation in the melt on the rate of supply of molecules to the growing crystal face of a lamella, and thereby gain considerable insight into the dependence of the overall growth process on molecular weight.

The observable crystal growth rate is, in general, a

result of two factors, the first being the nucleation rate of initiating stems on the substrate, and the second being the rate of coverage of the substrate by new stems that begin at the initial stem. Both of these processes suffer retardations from the fact that the long polymer molecules must somehow be extracted from the melt. In an earlier work<sup>5,6</sup> it was shown that it was reasonable to suppose that reptation (curvilinear diffusion) was the mechanism that allowed the force of crystallization readily to extract a rather long molecule from the melt and permit it, or some part of it, to fold down onto the crystal surface thus completing a portion of the substrate. Here, we shall improve and extend this treatment and apply it to polyethylene fractions crystallizing in both régimes I and II. The result is that the introduction of the concept of reptation together with other concepts inherent in nucleation theory leads to a quite satisfactory explanation of the absolute growth rate of polyethylene lamellae over a considerable range of molecular weight and temperature. At the same time it will become evident that reptation is the process that permits a molecule to be removed from the interentangled melt by the force of crystallization and to be pulled onto the growth front.

The pattern of the paper is as follows. First, the

phenomenological relationships governing the rate of crystallization in régimes I and II are examined to determine if the substrate completion rate,  $g$ , can be determined (or at least bounded) strictly on the basis of the experimentally-known crystallization rates without any input that is dependent upon the molecular details of nucleation theory. It is found that  $g$  is a simple function of certain known constants, i.e. the observed growth rate  $G_{I,II}$  at the régime I→régime II transition, and the substrate length  $L$ . Thus, it is possible to obtain an estimate of the 'experimental' substrate completion rate  $g_{expt}$ .

The next stage in the paper involves the development of the theoretical expressions based on nucleation theory for the absolute growth rate of régime I and régime II crystallization with the effect of reptation included. The theory has been deliberately kept simple, so that its physical basis is not obscured. The general result is that reptation causes a lowering of the observed growth rate with increasing molecular weight in both régimes, a prediction that is shown by the experiments on polyethylene to be correct. The rate  $g_{nuc}$  of the substrate completion process can be estimated from nucleation theory, and is roughly comparable to  $g_{expt}$ . Alternative expressions for the rate of substrate completion (denoted  $g_1$  and  $g_2$ ) are derived by calculating the reptation rate commensurate with the force of crystallization as it acts on a molecule subject to the known friction coefficient associated with reptation in the melt. These estimates of  $g$  prove to be in approximate accord with  $g_{nuc}$  and  $g_{expt}$ , allowing the conclusion to be drawn that reptation in the melt is fast enough to permit a substantial degree of 'regular' or 'tight' folding.

Some of the results, most particularly the pre-exponential factors in the expressions for the growth rate, are highly sensitive to the temperature  $T_m^\circ(\infty)$  that is chosen as the melting point of the infinite polyethylene crystal. This occurs because a small shift in  $T_m^\circ(\infty)$  implies a large change in the undercooling,  $\Delta T$ , if the crystallization temperature is near  $T_m^\circ(\infty)$ , as happens in the case of polyethylene. The value of  $T_m^\circ(\infty)$  for polyethylene is disputed, the estimates ranging from 141.4° to 145.5° ± 1°C (see later). To maintain the broadest possible base for the application of the theory, we have analysed the growth rate data on polyethylene fractions using a set of  $T_m^\circ(\infty)$  values ranging from 141.5° to 146.5°C. Highly satisfactory results are obtained from  $T_m^\circ(\infty)$  values ranging from ~142.5° to ~145°C, which allows the physical basis of the theory to be appreciated without being obfuscated by the aforementioned dispute.

The approach and analysis given in this paper provided information on topics such as the lateral surface free energy  $\sigma$ , and one parameter of considerable morphological interest, namely, the effective size of the substrate,  $L$ . The analysis carried out here permits a somewhat more detailed check on régime I and régime II theory than was practicable before. In particular, we have examined in more detail the change of slope at the régime I→régime II transition of plots of  $\log_{10} G + Q_b^*/2.303RT$  against  $1/T(\Delta T)$  which régime theory places at a factor of two. This is confirmed experimentally within rather narrow limits for the range of  $T_m^\circ(\infty)$  values noted above.

In summary, the present work emends nucleation theory to account for the effect of reptation on both the primary nucleation and substrate completion processes, and tests that theory using data for polyethylene fractions. The

result is that one then has a better conceptual picture of how chain-folded lamellae are formed from the melt, including some details of the manner in which the force of crystallization can draw a long pendant molecule, or some part thereof, out of the interentangled melt onto the substrate.

## THEORY

*Method of estimating substrate completion rate  $g$  from experimental crystallization rate data*

It is useful first to mention the phenomenological relationships that govern régime I and régime II behaviour (see *Figure 1*). For régime I where one primary nucleation act (occurring sporadically in time) causes the rapid completion of the entire substrate of length,  $L$ , we have<sup>1,7</sup>:

$$G_I = b_0 i L = b_0 i n_s a_0 \quad (1)$$

and for régime II, where multiple nucleation on the substrate occurs<sup>1,7,8</sup>:

$$G_{II} = b_0 (2 i g)^{1/2} \quad (2)$$

Here  $G$  represents the growth rate in  $\text{cm s}^{-1}$ ;  $b_0$  is the thickness of the layer or patch being added;  $i$  is the surface nucleation rate in nuclei  $\text{s}^{-1} \text{cm}^{-1}$ ;  $L = n_s a_0$ , the length of the substrate in cm;  $n_s$  is the number of stems of width  $a_0$  that make up this length; and  $g$  is the substrate completion rate in  $\text{cm s}^{-1}$  (*Figure 1*). The value of  $g$  given in equation (2) is the velocity in one direction.

At the transition between régimes I and II the observable crystallization rates for both are identical<sup>1,9</sup>, i.e.  $G_I = G_{II} = G_{I,II}$ . Under this condition it is seen from equations (1) and (2) that:

$$g_{expt} = \frac{G_{I,II} L}{2 b_0} = \frac{G_{I,II} n_s a_0}{2 b_0} \quad (3)$$

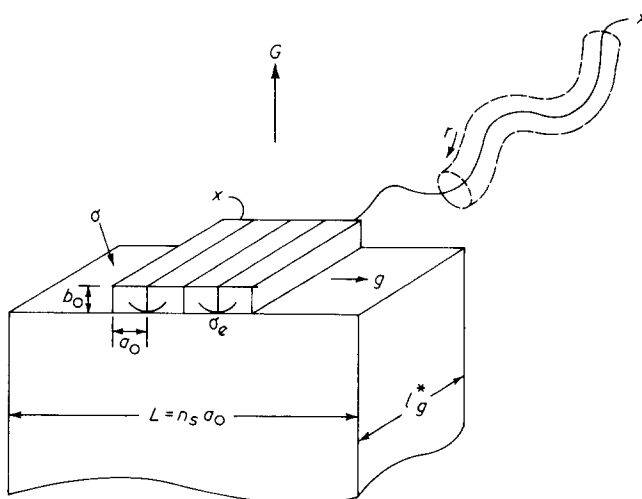


*Figure 1* Surface nucleation and substrate completion with reptation (schematic). The case shown refers to régime I where one surface nucleus deposited at rate  $i$  causes completion of substrate of length  $L$ , giving overall growth rate  $G_I = b_0 i L$ . Multiple surface nuclei occur in régime II (not shown) and lead to  $G_{II} = b_0 (2 i g)^{1/2}$ , where  $g$  is the substrate completion rate. The substrate completion rate,  $g$ , is associated with a 'reeling in' rate  $r = (l_g^*/a_0)g$  for the case of adjacent re-entry

Thus, we can obtain the value of  $g_{\text{expt}}$  at the transition temperature experimentally if values of  $G_{\text{I,II}}$ ,  $b_0$  and  $L$  are known. It is not necessary to know the theoretical form of  $i$  or  $g$ , which depend on a more detailed molecular picture, to make such estimates. The value of  $b_0$  is known from X-ray diffraction data, and values of  $G_{\text{I,II}}$  can readily be obtained from data on polyethylene fractions. Since it will emerge later that the absolute growth rate is approximately an inverse function of molecular weight as a result of reptation, it will prove convenient to write  $G_{\text{I,II}}$  in the form:

$$G_{\text{I,II}} = Y/n \quad (4)$$

where  $n$  is the number of units in the polymer chain. (Later it will be seen that  $n$  refers to an average length that is close to  $n_z$ , the number of chain units associated with the molecular weight  $M_z$ ). Then we find:

$$g_{\text{expt}} = \frac{YL}{2nb_0} = \frac{Yn_s a_0}{2nb_0} \quad (5a)$$

where  $Y$  is a constant to be determined experimentally from the  $G_{\text{I,II}}$  data on a set of fractions of known  $n$ . Observe that  $g_{\text{expt}}$  measures the substrate completion rate irrespective of whether or not the stems being added involve adjacent re-entry chain folds.

It will prove useful as a guide to what follows to give the value of  $Y$  obtained from experiments on polyethylene fractions  $n_z \cong 1900$  to  $n_z \cong 14\,500$  so that some bounds can be placed on  $g_{\text{expt}}$  at this stage of the treatment. For nine specimens in this range we find from the experimental  $G_{\text{I,II}}$  values at the régime transition, which is near 400K, that  $Y \cong 3.26 \times 10^{-3} \text{ cm s}^{-1}$ . (The standard deviation in  $Y$  is  $0.5 \times 10^{-3} \text{ cm s}^{-1}$ .) Then with  $b_0 = 4.15 \times 10^{-8} \text{ cm}$ , it is found from equation (4) that:

$$g_{\text{expt}} \cong 3.94 \times 10^4 L/n_z \quad (5b)$$

Thus, the burden of estimating the actual value of  $g_{\text{expt}}$  rests mostly with obtaining an estimate of the substrate length  $L$ . It is sufficient at this juncture to suppose that the  $L$  is perhaps 0.1 to 0.5  $\mu\text{m}$ , which gives  $g_{\text{expt}}$  from equation (5) as being  $\sim 0.40/n_z$  to  $\sim 2.0/n_z$  at  $T \cong 400\text{K}$ . This corresponds to a range of  $g = 5.6 \times 10^{-5}$  to  $2.8 \times 10^{-4} \text{ cm s}^{-1}$  for a pendant chain  $M_z = 10^5$ . This accords closely with an earlier 'experimental' estimate of  $g_{\text{expt}} \cong 1 \times 10^{-4} \text{ cm s}^{-1}$  for this molecular weight, calculated from  $g_{\text{expt}} \cong 0.70/n$  that was obtained by a more complicated procedure<sup>6,10</sup>. Subsequently, we shall note the estimates of  $L$  that derive strictly from the kinetics of crystallization, as well as the upper bound for this quantity suggested by experiment.

The value of  $n$  used in equations (4), (5a) and (5b) was taken to correspond to the full molecular length as measured by  $n_z = M_z/14$ . The actual pendant chain in both régimes I and II will have a true number of chain units that is somewhat less than  $n_z$  because the nucleating chain will attach to the substrate somewhere along its length leaving (in the average case) two pendant chains of unequal length. The longer of these will tend to control the crystallization properties. The mean initial length of the longer pendant chain will be within a factor of about 2/3 of the full chain length, and to the approximation given here we do not correct for this effect.

The importance of the substrate completion rate in the present problem is partly a result of the fact that  $g$  is related to the 'reeling in' or reptation rate  $r$  according to<sup>5,6</sup>:

$$r = \left( \frac{l_g^*}{a_0} \right) g \quad (6)$$

where  $r$  is the reptation rate in  $\text{cm s}^{-1}$ ;  $l_g^*$  is the thickness of the chain-folded lamella; and  $a_0$  is the width of a stem on the substrate. The origin of equation (6) is readily seen in Figure 1. Notice that equation (6) assumes that the entire pendant molecule is reeled in a regularly folded manner; the implications of this assumption will be noted later. It is clear from the foregoing discussion that an experimental estimate of  $r$  can be obtained from values of  $g$  derived from experimental crystallization rates. The value of  $r_{\text{expt}}$  so obtained can then be compared with theoretical estimates. (From previous work<sup>6,10</sup>, we had estimated the value  $r_{\text{expt}} \cong 30.7/n \text{ cm s}^{-1}$  at  $T \cong 400\text{K}$ . If we take  $g_{\text{expt}}$  as  $0.4/n$ , which corresponds to the assumption  $L = 0.1 \mu\text{m}$ , then the present work suggests through equations (5b) and (6) that  $r_{\text{expt}} \cong 17/n_z$ .) The theoretical estimates arise from two sources. One formula for  $g$  derives straight away from nucleation theory modified to account for the presence of reptation; we then obtain  $r$  through equation (6). The second approach involves a direct calculation of the rate of 'reeling-in',  $r$ , based on the known friction coefficient of reptation  $\zeta_r$  as it interacts with the mean force of crystallization,  $\bar{f}_c$ , as calculated using two approximations. These rates will be denoted  $r_1$  and  $r_2$ . A comparison of the experimental value of the reptation rate estimated from crystallization rates in régimes I and II for polyethylene fractions with that obtained from nucleation theory and the friction coefficient methods will serve to show that the reptation concept explains important features of the crystallization process, and further, that the reptation process in the melt is rapid enough to permit a substantial degree of regular chain-folding.

*Development of nucleation theory formulae for  $G_{\text{I}}(T)$ ,  $G_{\text{II}}(T)$  with reptation: Estimate of absolute pre-exponential factors*

The nucleation rate  $i$  in nuclei (stems of width  $a_0$ ) per substrate length  $L = a_0 n_s$  per second is given by:

$$i(\text{nuclei cm}^{-1} \text{ s}^{-1}) = S_T/a_0 n_s \quad (7)$$

where, as in previous work<sup>1,6</sup>, the total flux is:

$$S_T = \frac{1}{l_u} \int_{2\sigma_e/(\Delta f)}^{\infty} S(l) dl \quad (8)$$

In this expression  $l_u$  is the length of a monomer unit in  $\text{cm}$ , and  $\sigma_e$  the fold surface free energy,  $q/2a_0 b_0$ , in  $\text{erg cm}^{-2}$  where  $q$  is the work or chain-folding. The expression for  $S(l)$  is<sup>1,9</sup>:

$$S(l) = N_0 A_0 (A - B)/(A - B + B_1) \quad (9)$$

where the elementary process rate constants may be written<sup>1,6</sup>:

$$A_0 = \beta_g \exp[-2b_0 \sigma_l / kT + \psi a_0 b_0 l(\Delta f) / kT] \quad (10)$$

$$\mathbf{B}_1 = \beta_g \exp[-(1 - \psi a_0 b_0 l (\Delta f) k T)] \quad (11)$$

$$\mathbf{A} = \beta_g \exp[-q/kT + \psi a_0 b_0 l (\Delta f)/kT] \quad (12)$$

$$\mathbf{B} = \beta_g \exp[-(1 - \psi) a_0 b_0 l (\Delta f) k T] \quad (13)$$

In these latter formulae,  $\beta_g$  is a retardation parameter that represents the resistance in the melt of the molecule being pulled onto the substrate, including its activation energy, and  $\psi$  is a parameter between zero and unity that weights the forward and backward reactions. There is good reason to believe (see later) that  $\psi$  will have values rather nearer zero than unity. The quantity  $N_0$  is the number of reacting species at the growth front. This leads directly to:

$$i = S_T/a_0 n_s = \left( \frac{N_0 \beta_g p_i}{a_0 n_s} \right) \exp[-4b_0 \sigma \sigma_e / (\Delta f) k T] \quad (14)$$

where

$$p_i = kT/2l_u b_0 \sigma \quad (15)$$

Here  $\Delta f = (\Delta h_f)(\Delta T)/T_m^\circ$ , where  $\Delta T$  is the undercooling. It will be seen later that  $p_i$  is a number that generally falls between 5 and 10.

We must now decide on expressions for  $\beta_g$  and  $N_0$ . In the case of  $\beta_g$ , which is in events per second, we use as before<sup>6</sup>:

$$\beta_g = (\kappa/n)(kT/h) \exp[-Q_D^*/RT] \quad (16)$$

where  $Q_D^*$  is the activation energy for the reptation process. The factor  $1/n$  is intended to represent the effect of chain length on the reptation rate in the melt. Equation (16) is arranged so that when  $Q_D^* \rightarrow 0$  and  $n \rightarrow 1$ ,  $\beta_g$  approaches a frequency factor of the order of magnitude of  $kT/h$ . The numerical factor  $\kappa$  can be determined from experiment, and should be within an order of magnitude of unity if equation (16) is properly constructed. In the most ideal case,  $\kappa$  would represent the number of chain units that act as the effective segment length in the liquid state, which would place it at 5 to 10. In the analysis of data, we shall in any case reject  $\kappa$  values that exceed 10. Subsequently, we shall further justify the general form of equation (16) by the use of reptation theory.

It will prove useful in what follows to make an estimate of the theoretical value of  $N_0$  in equations (9) and (14). This is difficult to do exactly, but reasonable estimates can be made. The absolute value of  $N_0$  is of some importance in estimating  $L$  and  $n_s$  from strictly kinetic data.

We first introduce the concept that  $N_0$  is proportional to the number of  $-\text{CH}_2-$  units on the growth front. This leads to a factor  $\bar{z} n_s$ , where  $\bar{z}$  is the number of  $-\text{CH}_2-$  units corresponding to the lamellar thickness  $l_g^*$ , and  $n_s$  is the number of stems in the substrate  $L$ . Further, the absolute value of  $N_0$  will contain a coordination factor  $C_n$  which we shall take to be between 4 and 6, that represents the number of  $-\text{CH}_2-$  units on the surface to which a  $-\text{CH}_2-$  unit in the melt attaches. Finally, we introduce a numerical factor  $P_0$  that represents the *configurational path degeneracy* (CPD) involved in the initial stem attachment process. In the simplest case, where the stems are represented as attaching to the surface as a unit with no fluctuations in length, we would set  $P_0 \sim 1$ . In the more realistic case where fluctuations in stem length about  $l_g^*$  are considered, as has been done by Lauritzen and Passaglia<sup>11</sup> (see also comments by Point<sup>12</sup>), we must expect  $P_0 > 1$ . The case  $P_0 > 1$  arises fundamentally from

the fact that there are a large number of crystallization paths<sup>13</sup>. The analysis given later will be carried out with  $P_0 = 1$  and  $P_0 = 25$ . These represent reasonable bounds for the CPD, and lead to a successful analysis. The upper bound in particular should be regarded as approximate. The foregoing developments lead to:

$$N_0 = (\bar{z} n_s) C_n P_0 \quad (17)$$

Equation (17) differs from a previous formulation, and in our opinion represents a better approximation for  $N_0$ .

With the foregoing it is found that:

$$i(\text{nuclei cm}^{-1} \text{ s}^{-1}) = (p_i \bar{z}/a_0)(C_n P_0)(\kappa/n)(kT/h) \times \exp[-Q_D^*/RT] \exp[-4b_0 \sigma \sigma_e / (\Delta f) k T] \quad (18)$$

With this expression one can then use equation (1) to obtain the absolute growth rate for régime I, which is:

$$G_1 = b_0 i n_s a_0 = \left( \frac{C_1}{n} \right) \exp[-Q_D^*/RT] \times \exp[-4b_0 \sigma \sigma_e / (\Delta f) k T] \quad (19)$$

where

$$C_1 = \kappa p_i (kT/h)(C_n P_0) b_0 (\bar{z} n_s) \quad (20)$$

The expression for  $G_1$  can be written in the general form:

$$G_1 = (C_1/n) \exp[-Q_D^*/RT] \exp[-K_{g(1)}/T(\Delta T)] \quad (21)$$

where

$$K_{g(1)} = 4b_0 \sigma \sigma_e T_m^\circ / (\Delta h_f) k \quad (22)$$

The factor  $C_1/n$  replaces the constant pre-exponential  $G_{0(1)}$  in other formulations.

Notice that the pre-exponential factor  $C_1/n$  falls as  $1/n$  because of the effect of reptation. Thus, in this formulation, an increase of molecular weight at a given undercooling  $\Delta T$  will depress the absolute growth rate. The present treatment of régime I differs in this respect from an earlier one<sup>6</sup>, though the exponential factors are identical.

The quantity  $Q_D^*$  is known for polyethylene from the work of Klein and Briscoe<sup>14</sup> to be  $7000 \text{ cal mol}^{-1}$  ( $29310 \text{ J mol}^{-1}$  on the basis  $1 \text{ cal} = 4.187 \text{ J}$ ). The value of the exponent  $K_{g(1)} = 4b_0 \sigma \sigma_e T_m^\circ / (\Delta h_f) k$  and  $C_1$  can therefore be obtained with sufficient accuracy from rate of crystallization data on polyethylene fractions from plots of  $\log_{10} G_1 + 7000/2.303RT$  against  $1/T(\Delta T)$  provided that  $T_m^\circ$  is known. The value of  $\sigma \sigma_e$  can be readily computed from the known value of  $K_{g(1)}$ .

We turn now to the calculation of the absolute growth rate for régime II. It is seen from equation (2) that this requires a theoretical expression for  $g$  as well as  $i$ . As in an earlier analysis<sup>6</sup>, we can obtain  $g$  directly from nucleation theory as<sup>1,9</sup>:

$$g \equiv a_0(\mathbf{A} - \mathbf{B}) = a_0 \beta_g \{ \exp[-q/kT] - \exp[-a_0 b_0 l (\Delta f)/kT] \} \quad (23)$$

for the case  $\psi = 0$ . With the substitution  $l = l_g^* = 2\sigma_e / (\Delta f) + kT/b_0 \sigma$  where  $\sigma_e = q/2a_0 b_0$  there is obtained:

$$g = a_0 \beta_g \exp[-q/kT] \{1 - \exp[-a_0(\Delta f)/\sigma]\} \quad (24)$$

or to an approximation sufficient for many purposes we may write:

$$g_{nuc} = g \cong a_0 (\kappa/n) f(kT/h) \exp[-Q_D^*/RT] \exp[-q/kT] \quad (25)$$

where we have expanded the exponential in the last factor in equation (24) to obtain the approximation

$$f \cong a_0 (\Delta f)/\sigma = a_0 (\Delta h_f) (\Delta T)/\sigma T_m^\circ \quad (26)$$

The value of  $f$  is fairly close to  $1/2$  for polyethylene in the temperature range of interest. The symbol  $g_{nuc}$  in equation (25) denotes that the value of the substrate completion rate calculated in this manner derives from nucleation theory. The bulk of the stems that comprise a lamella enter it during substrate completion.

Observe from equation (25) that according to nucleation theory the substrate completion process is controlled by two mechanisms. The first is reptation in the melt, which is represented by the factor  $(1/n) \times \exp(-Q_D^*/RT)$ , and the second is the process of forming a chain-fold, which is represented by the factor  $\exp(-q/kT)$ . It is clear on general physical grounds that both factors must be present.

It may be noted in passing that had we chosen the case  $\psi = 1$  for consideration the factor  $\exp(-q/kT)$  would not have appeared<sup>1</sup> at all in  $g$ . For this reason alone, we may regard the case  $\psi = 1$  as invalid from a theoretical point of view, and we have restricted ourselves accordingly to low values of this parameter. The 'delta catastrophe', wherein a very large value of the initial thickness  $l_g^*$  suddenly occurs at a large undercooling, is avoided when low  $\psi$  values are employed. This sudden increase of  $l_g^*$  at large undercoolings has not been observed experimentally<sup>15,16</sup>. Values of  $\psi$  ranging from zero to about  $1/3$  give good agreement with lamellar thickness data<sup>1</sup>.

It is now a simple matter to set down the absolute growth rate for régime II as:

$$G_{II} = b_0 (2ig)^{1/2} = \left(\frac{C_{II}}{n}\right) \exp[-Q_D^*/RT] \times \exp[-2b_0 \sigma \sigma_e / (\Delta f) kT] \quad (27)$$

where:

$$C_{II} (2p_f f)^{1/2} (C_n P_0)^{1/2} \kappa (kT/h) b_0 \bar{z}^{1/2} \exp[-q/2kT] \quad (28)$$

The expression for  $G_{II}$  can be written as:

$$G_{II} = (C_{II}/n) \exp[-Q_D^*/RT] \exp[-K_{g(II)}/T(\Delta T)] \quad (29)$$

where

$$K_{g(II)} = 2b_0 \sigma \sigma_e T_m^\circ / (\Delta h_f) k \quad (30)$$

where  $C_{II}/n$  replaces  $G_{0(II)}$  in earlier formulations. Observe that  $K_{g(II)} = 2K_{g(II)}$  according to régime theory<sup>1,7</sup>. This leads to a change of slope of 2 in plots of  $\log_{10} G + Q_D^*/2.303RT$  against  $1/T(\Delta T)$  as one passes

through the régime transition at  $T_t$ . The values of  $C_{II}$  and  $K_{g(II)}$  can readily be obtained from the appropriate plots of régime II data, and values of  $\sigma \sigma_e$  calculated from  $K_{g(II)}$  once a value of  $T_m^\circ$  ( $\infty$ ), which decides  $\Delta T_t$ , is assumed.

The exponential terms involving  $Q_D^*/RT$  and  $K_{g(II)}$  in equation (29) are similar to those found in previous treatments of régime II<sup>1,6,17</sup>. However, with the concept of reptation being introduced into both  $i$  and  $g$  according to equation (16), the pre-exponential factor  $G_{0(II)} = C_{II}/n$  for régime II now falls as  $1/n$ .

The general picture of régime I and régime II crystallization predicted by the present treatment is shown in Figure 2 for input parameters relevant to the case of polyethylene. A plot of  $\log_{10} G$  against  $T$  (not shown) would exhibit crossovers at the lower molecular weights because of the lower  $T_m^\circ$  values associated with these molecular weights. The régime transition takes place at the same undercooling for each molecular weight

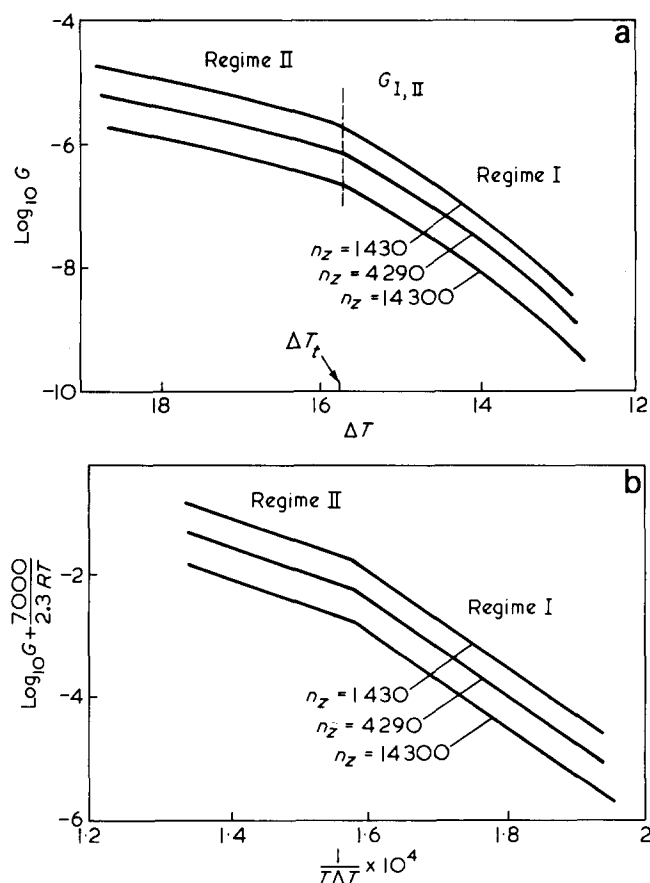


Figure 2 Theoretical plots of  $\log_{10} G$  versus  $\Delta T$  and  $\log_{10} G + 7000/2.303 RT$  versus  $1/T(\Delta T)$  in vicinity of régime I  $\rightarrow$  régime II transition, showing predicted reduction in growth rate  $G$  with increasing  $n_z$  caused by reptation.  $G$  in  $\text{cm s}^{-1}$  calculated with equations (19)–(22) and (27)–(30) for  $n_z = 1430, 4290$ , and  $14300$  using  $T_m^\circ(\infty) = 145^\circ \text{C}$ ,  $C_1 = 5.00 \times 10^{13}$ ,  $C_{11} = 3.34 \times 10^7$ ,  $K_{g(II)} = 0.900 \times 10^5 \text{ deg}^2$ ,  $K_{g(I)} = 1.800 \times 10^5 \text{ deg}^2 = 2K_{g(II)}$ , and  $Q_D^* = 7000 \text{ cal mol}^{-1}$ . With  $b_0 = 4.15 \times 10^{-8} \text{ cm}$  and  $\Delta h_f = 2.8 \times 10^9 \text{ erg cm}^{-3}$ , the  $K_g$  values both give  $\sigma \sigma_e = 1010 \text{ erg}^2 \text{ cm}^{-4}$ . With  $\sigma_e = 90 \text{ erg cm}^{-2}$ , this yields  $\sigma = 11.2 \text{ erg cm}^{-2}$ . The assignment of  $C_1$ ,  $C_{11}$ , and  $K_{g(I)} = 2K_{g(II)}$  fixes  $\Delta T_t$  at  $15.8^\circ \text{C}$ , which is close to the experimental value of  $16^\circ \pm 1^\circ \text{C}$ . The  $C_1$  and  $C_{11}$  values with  $C_n = 4$ ,  $P_0 = 25$ ,  $\bar{z} = 150$ ,  $l_U = 1.27 \times 10^{-8} \text{ cm}$ ,  $a_0 = 4.55 \times 10^{-8} \text{ cm}$  and  $q = 4900 \text{ cal mol}^{-1}$  imply  $n_s = 2.42 \times 10^2$  (i.e.  $L = 0.11 \mu\text{m}$ ) from equation (32) and  $\kappa = 8.67$  from either equation (20) or (28). The value of  $\kappa$  cited scales the absolute values of  $G_I$  and  $G_{II}$  so that they almost exactly match the experimental results for polyethylene (see Figure 3)

as shown, but the transition temperature falls as the molecular weight is lowered, which leads to the crossover.

The ratio  $C_I/C_{II}$  can be determined experimentally for polyethylene fractions, and is of special interest because it leads to an estimate of the number of stems in the substrate  $n_s$  (and hence the substrate length  $L$ ) that is independent of  $\kappa$  and  $n$ . From the foregoing, we see that the ratio  $C_I/C_{II}$  has the value:

$$C_I/C_{II} = (p_i/2f)^{1/2} (C_n P_0)^{1/2} \bar{z}^{1/2} n_s \exp[q/2kT] \quad (31)$$

which gives

$$n_s = \left(\frac{2f}{p_i}\right)^{1/2} (C_n P_0)^{-1/2} \left(\frac{C_I}{C_{II}}\right) \bar{z}^{-1/2} \exp[-q/2kT] \quad (32)$$

With the ratio  $C_I/C_{II}$  known from experiment, together with the close estimates of  $\bar{z}$  and  $q$  that are available, and noting that the quantity

$$\left(\frac{2f}{p_i}\right)^{1/2} = 2[a_0 b_0(\Delta f) l_w / kT]^{1/2} \quad (33a)$$

can be calculated with considerable accuracy (it has a value of roughly 1/2 in the range of interest), it is readily seen that  $n_s$  can be estimated from kinetic data. However, there are two factors that render the value of  $n_s$  calculated from equation (32) somewhat uncertain. Foremost among these is that the experimental value of the ratio  $C_I/C_{II}$  depends on the melting point chosen for polyethylene, and this quantity is the subject of some dispute. The other is that  $n_s$  depends on  $(C_n P_0)^{-1/2}$ , which with  $P_0$  varying between 1 and 25, introduces an initial uncertainty of 5. Nevertheless, these difficulties can be overcome to a considerable extent, as will be shown in the treatment to follow. It was pointed out previously<sup>17</sup> that the ratio of pre-exponential factors for regimes I and II was a measure of the substrate length, though the present treatment is considerably more exact.

We observe finally that the foregoing treatment leaves the initial lamellar thickness unchanged from previous calculations, and to a sufficient approximation for present purposes this quantity takes on the value:

$$l_g^* \cong 2\sigma_e / (\Delta f) + kT / b_0 \sigma \quad (33b)$$

A more exact expression for the second term on the right-hand-side, commonly called  $\delta l$ , may be found elsewhere<sup>1</sup>. A crystal of thickness  $2\sigma_e / (\Delta f)$  would melt at its crystallization temperature, but one of thickness  $2\sigma_e / (\Delta f) + \delta l$  is stable at that temperature<sup>1</sup>.

*Alternative method of calculation of g and r from the friction coefficient of reptation in the melt and the force of crystallization*

In one approximation, the rate at which a pendant molecule can be drawn onto the substrate by the force of crystallization associated with a lamella of finite thickness  $l_g^*$  with folds on its surface, which force acts against a resistance resulting from reptation in the melt, has been treated previously<sup>5,6</sup>. In brief, the mean force of crystallization calculated as being proportional to the 'smoothed' derivative of the free energy of formation with

respect to the dimension along the substrate is given for such a crystal by:

$$\bar{f}_{1(c)} = (\delta l / l_g^*) a_0 b_0 (\Delta f) \quad (34)$$

where to a sufficient approximation

$$\delta l \cong kT / b_0 \sigma \quad (35)$$

The factor  $a_0 b_0 (\Delta f)$  represents the force exerted on a pendant chain by a crystal exclusive of the region just at the chain-fold. Now according to DiMarzio *et al.*<sup>5</sup>, the diffusion coefficient  $D_r$  and friction coefficient  $\zeta_r$  for reptation are related according to:

$$D_r = 3 D_{CM} \langle \mathcal{L}^2 \rangle / \langle R^2 \rangle = kT / \zeta_r = kT / \zeta_0 n \quad (36)$$

where  $\langle \mathcal{L}^2 \rangle$  is the average value of the square of the contour length,  $\langle R^2 \rangle$  is the average value of the square of the end-to-end distance, and  $D_{CM}$  is the customary experimentally-measured centre-of-mass diffusion coefficient. It is known that  $D_{CM}$  varies with  $n$  as  $D_{CM} = D_0 / n^2$  for polyethylene;  $D_0$  is known from the same experiments. Thus, we have for the friction coefficient for reptation as predicted by reptation theory the expression<sup>5,6</sup>:

$$\zeta_r = \zeta_0 n = kT / D_r = (kT / 0.305 D_0) n \quad (37)$$

The value of  $D_0$  depends on temperature in a manner proportional to  $\exp(-Q_D^*/RT)$ . The value of  $D_0$  is  $0.51 \times 10^{-3} \text{ cm}^2 \text{ s}^{-1}$  at the reference temperature  $T_0 = 400\text{K}$  for polyethylene<sup>6,10</sup> and it is found that  $\zeta_0$  at the same temperature is  $\zeta_0 = 3.56 \times 10^{-10} \text{ erg s cm}^{-2}$ . Hence, the velocity of reptation in this instance is<sup>6</sup>:

$$r_1 = v_{r,q} = \bar{f}_{1(c)} / \zeta_r = (\delta l / l_g^*) a_0 b_0 (\Delta f) / \zeta_0 n = \frac{(\delta l / l_g^*) a_0 b_0 (\Delta f)}{(kT / 0.305 D_0) n} \quad (38)$$

The corresponding formula for  $g$  is

$$g_1 = g_{r,q} = r_1 \left(\frac{a_0}{l_g^*}\right) = \frac{(a_0 / l_g^*) (\delta l / l_g^*) a_0 b_0 (\Delta f)}{\zeta_0 n} = \left(\frac{a_0}{l_g^*}\right) \frac{(\delta l / l_g^*) a_0 b_0 (\Delta f)}{(kT / 0.305 D_0) n} \quad (39)$$

The notation  $r_{r,q}$  and  $g_{r,q}$  refers to that used in previous work<sup>6</sup>.

It will provide additional insight to give another approach to the calculation of the mean force on the crystallizing chain, which takes into account the fact that no force is exerted on the reptating chain during fold formation, whereas the maximum force  $a_0 b_0 (\Delta f)$  is exerted during stem formation. Accordingly we assume that the residence times and forces exerted during stem and fold formation are:

$$t_{\text{stem}} = \tau_0 l_g^* ; \quad \text{Force} = a_0 b_0 (\Delta f) \quad (40a)$$

$$t_{\text{fold}} = \tau_0 l_f \exp[q/kT] ; \quad \text{Force} = 0 \quad (40b)$$

where  $\tau_0$  is the unit of time involved in putting down one monomer unit, and  $l_f$  the length of a fold. Then the time-average mean force is:

$$\begin{aligned} \bar{f}_{2(c)} &= \left( \frac{\tau_0 l_g^*}{\tau_0 l_g^* + \tau_0 l_f \exp[q/kT]} \right) a_0 b_0 (\Delta f) \\ &\cong (l_g^*/l_f) a_0 b_0 (\Delta f) \exp[-q/kT] \end{aligned} \quad (41)$$

since  $l_f \exp(q/kT) \gg l_g^*$ . With this we have the mean reptation rate:

$$r_2 = f_{2(c)} / \zeta_0 n = \frac{(l_g^*/l_f) a_0 b_0 (\Delta f) \exp[-q/kT]}{\zeta_0 n} \quad (42)$$

The corresponding substrate completion rate calculated as  $g_2 = r_2 (a_0/l_g^*)$  is:

$$g_2 = \frac{(a_0/l_f) a_0 b_0 (\Delta f) \exp[-q/kT]}{\zeta_0 n} \quad (43)$$

We note that the temperature dependence of  $\zeta_0$  implies a factor  $\exp(-Q_D^*/kT)$  in both  $g_1$  and  $g_2$ , so that it is clear that a general resemblance exists between equation (25) for  $g$  as derived from nucleation theory, and the above expressions for  $g_1$  and  $g_2$ . This point will be discussed in some detail later.

All of the quantities in equations (38) and (39), and (42) and (43) can be determined with sufficient accuracy to obtain a reasonable estimate of  $r_1$ ,  $r_2$ ,  $g_1$ , and  $g_2$ . The importance of these calculations is that they give the magnitude of the reptation velocity, and hence the substrate completion rate, that can be sustained by the friction coefficient for this process in the melt as it is perturbed by the force of crystallization.

One test that we shall be interested in is the comparison of  $r_1$  and  $r_2$ , and both of the corresponding quantities  $g_1$  and  $g_2$  calculated using the 'regular fold' assumption  $g = (a_0/l_g^*)r$ , with the value of  $g_{nuc}$  as calculated from nucleation theory according to equation (25). A relatively close correspondence between  $g_1$  and  $g_2$  on the one hand and  $g_{nuc}$  on the other would tend to validate our theoretical approaches. It will be shown subsequently that  $g_{nuc}$  and  $g_2$  in particular have in fact a quite similar physical basis, so at least a fair degree of agreement can be anticipated. We shall of course also be interested in how  $g_1$  compares numerically with  $g_2$ . Finally, we shall be interested in how all of the above quantities compare with  $g_{expt}$ . If  $g_1$ ,  $g_2$  and  $g_{nuc}$  are approximately equal to or greater than  $g_{expt}$ , then it would follow that a significant degree of 'regular' or adjacent re-entry chain-folding could take place during substrate completion. Specifically, this would mean that a pendant molecule

could be reeled in fast enough with adjacent re-entry to be compatible with the observed growth rate. Conversely, if these quantities proved to be much less than  $g_{expt}$ , it would follow that the 'reeing in' process would be too slow to permit any significant degree of adjacent re-entry chain-folding. Values of  $g_1$ ,  $g_2$  or  $g_{nuc}$  that were somewhat lower than  $g_{expt}$  would imply that only a portion of the chain being reeled in experienced adjacent re-entry during substrate completion. This test will be carried out subsequently, with the result that the reptation process in polyethylene is found to be sufficiently rapid in the temperature range under consideration to allow the degree of adjacent or 'tight' folding that is believed to be present. The calculations for  $g_1$ ,  $g_2$ ,  $g_{nuc}$  and  $g_{expt}$  will be given for crystallization temperatures centring about  $T_x = T_m^\circ - \Delta T$ , which for the polyethylene fractions to be considered is always within a few degrees of 400K. At sufficiently lower crystallization temperatures, reptation will be impaired. This point will be discussed briefly.

## ANALYSIS OF GROWTH RATE DATA ON PE FRACTIONS

### Growth rate data on PE fractions

Considerable data have been amassed on the growth rate of polyethylene fractions of moderate to high molecular weight that clearly exhibit the régime I  $\rightarrow$  régime II transition<sup>17</sup>. Specimens of about  $M_w \cong M_z \cong 2 \times 10^4$  up to considerably higher molecular weights exhibit both régimes in sufficient detail to permit an analysis of the type contemplated here; the highest molecular weight fraction in our possession that clearly exhibited both régimes was  $M_z = 2.04 \times 10^5$ . Samples of higher molecular weight tended to have broader molecular weight distributions that obscured the régime effect. Accordingly, the nine fractions noted in Table 1 were chosen for the purpose at hand. Some typical plots of  $\log_{10} G$  against  $\Delta T$  are shown in Figure 3. The régime effect is especially clearly defined in the specimens of low and intermediate molecular weight.

Table 1 shows the temperature of the régime I  $\rightarrow$  régime II transition,  $T_t$ , and the value of  $G_{I,II}$  at  $T_t$ . (The  $G_{I,II}$  data given in the Table are those that were used to find the value of  $Y$  in equations (4) and (5).) Also shown is the melting point  $T_m^\circ$  for each fraction estimated on the basis of the melting point of an infinitely long chain crystal  $T_m^\circ(\infty)$ , being 145°C and 142°C, respectively. Values of  $T_m^\circ$  for the other choices of  $T_m^\circ(\infty)$  can be obtained by interpolation or extrapolation. Values of  $T_m^\circ(\infty)$  for polyethylene near these two values have been proposed in

Table 1 Properties of polyethylene fractions used in analysis

	$M_w$	$M_z$	$n_z$	$T_t$ (°C)	$G_{I,II}$ at $T_t$ (cm s <sup>-1</sup> )	$T_m^\circ$ for $T_m^\circ(\infty) =$ 145°C	$T_m^\circ$ for $T_m^\circ(\infty) =$ 142°C
1	23 600	26 500	1900	126.7	$2.69 \times 10^{-6}$	142.8	140.0
2	24 700	27 600	1980	126.6	$3.26 \times 10^{-6}$	142.9	140.0
3	30 000	35 300	2530	128.0	$8.51 \times 10^{-7}$	143.3	140.4
4*	30 000	35 300	2530	127.6	$1.07 \times 10^{-6}$	143.3	140.4
5	37 600	43 700	3130	127.3	$9.07 \times 10^{-7}$	143.6	140.7
6	42 600	53 400	3820	128.2	$1.55 \times 10^{-6}$	143.8	140.9
7	62 800	98 500	7040	128.6	$4.00 \times 10^{-7}$	144.2	141.3
8	74 473	85 900	6140	128.8	$2.16 \times 10^{-7}$	144.2	141.3
9	113 800	203 600	14 540	128.0	$2.27 \times 10^{-7}$	144.6	141.7

\* Duplicate run

the literature<sup>18-21</sup>. Some of our results, for example,  $C_I$  and  $C_{II}$ , are highly sensitive to the choice of  $T_m^\circ(\infty)$ . Accordingly, we adopt a strategy of using a range of  $T_m^\circ(\infty)$  values in the analysis, and apply criteria to be stated subsequently to select the best values of the

parameters given by the analysis. The melting point equation used to calculate  $T_m^\circ$  for each fraction is given in a previous publication<sup>17</sup>. Somewhat simplified, it is of the general form:

$$T_m^\circ(n) = [(a + bn)/(c + dn + R \ln n)] \quad (44)$$

where the factors  $a + bn$  and  $c + dn + R \ln n$  represent the enthalpy and entropy of melting, respectively, and  $a$ ,  $b$ ,  $c$  and  $d$  are constants. The value of  $T_m^\circ(\infty)$  is  $b/d$ , which can be set anywhere between 414.7K (141.5°C) to 419.7K (146.5°C). For the case  $T_m^\circ(\infty) = 145.5^\circ\text{C} = 418.7\text{K}$ , the melting points calculated with this expression closely approximate those found with the Flory-Vrij<sup>18</sup> treatment, which gives  $T_m^\circ(\infty) = 145.5 \pm 1^\circ\text{C}$ . The melting points of the n-alkanes were accurately reproduced for any value of  $T_m^\circ(\infty)$  within the quoted range.

Figure 3 shows a plot of  $\log_{10} G$  against  $\Delta T$  of the experimental data for several of the fractions. It is seen that the growth rate becomes lower in both régimes I and II as the molecular weight is increased, as predicted by equations (19)–(21) and (27)–(29), and as illustrated schematically in Figure 2. This decrease of  $G$  is a result of the  $1/n$  factor arising from reptation, as expressed in equation (16), in the nucleation and substrate completion process. This finding strongly supports in a general manner the nucleation theory approach proposed here.

*Analysis of data to obtain  $\sigma\sigma_e$  and the pre-exponential constants  $C_I$  and  $C_{II}$  for régimes I and II*

Plots of  $\log_{10} G + Q_b^*/2.303RT$  against  $1/T(\Delta T)$  were constructed for each fraction to obtain  $K_{g(I)}$  and  $K_{g(II)}$  as indicated by the theory, and analysed with equations (21)–(22) to obtain  $\sigma\sigma_e$  and  $C_I$  for régime I, and with equations (29)–(30) to obtain  $\sigma\sigma_e$  and  $C_{II}$  for régime II. Some typical plots are shown in Figure 3. The values of  $\sigma\sigma_e$  were calculated from the measured  $K_g$  values using  $\Delta h_f = 2.8 \times 10^9 \text{ erg cm}^{-3}$  (corresponding to 1000 cal mol<sup>-1</sup> or 4187 J mol<sup>-1</sup> or  $-\text{CH}_2^-$ ); and  $b_0 = 4.15 \times 10^{-8} \text{ cm}$ . Estimates of  $C_I$  and  $C_{II}$  were also found from plots such as are shown in Figure 3. Observe the resemblance of these plots to the schematic diagram in Figure 2. Values of  $C_I$ ,  $C_{II}$ , and  $\sigma\sigma_e$  obtained for various assumed values of  $T_m^\circ(\infty)$  are given in Table 2. The data noted in Table 2 for a given  $T_m^\circ(\infty)$  are the mean values for all the specimens listed in Table 1. The slopes for the régime I data are generally similar, and the same holds for the régime II slopes.

According to régime theory,  $K_{g(I)}$  should be equal to  $2K_{g(II)}$ , and the  $\sigma\sigma_e$  values computed from the two régimes

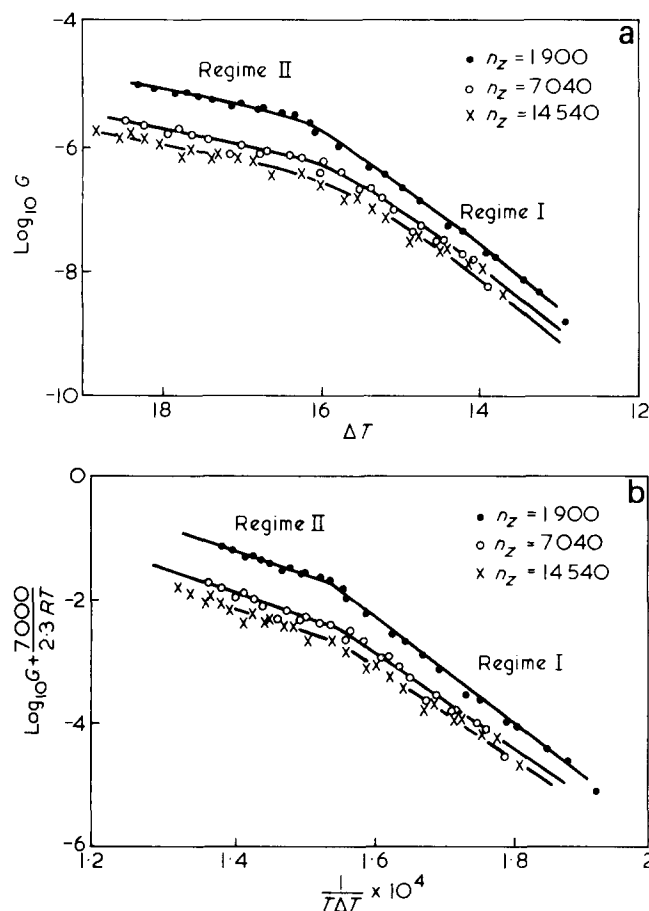


Figure 3 Experimental plots of  $\log_{10} G$  versus  $\Delta T$  and  $\log_{10} G + 7000/2.303 RT$  versus  $1/T(\Delta T)$  for polyethylene fractions  $n_z = 1900$ , 7040, and 14540.  $G$  is in  $\text{cm s}^{-1}$ , and  $\Delta T$  is calculated on the basis  $T_m^\circ(\infty) = 145.0^\circ\text{C}$

Note strong resemblance between theoretical calculations shown in Figure 2 and corresponding experimental plots shown in this Figure.

The values of  $K_{g(I)}$  and  $K_{g(II)}$  obtained directly from the data are  $1.857 \times 10^5$  and  $0.900 \times 10^5 \text{ deg}^2$ , respectively. The values  $C_I = 2.73 \times 10^{14}$  and  $C_{II} = 3.34 \times 10^7$  are also found directly from the data. These results imply  $\sigma\sigma_e = 1023 \text{ erg}^2 \text{ cm}^{-4}$ ,  $\sigma = 11.4 \text{ erg cm}^{-2}$ , and with  $P_0 = 25$ ,  $\kappa = 8.64$  and  $L = 0.6 \mu\text{m}$ . The small differences between the results quoted here and those noted in the legend of Figure 2 are caused by the fact that the constraint  $K_{g(I)} = 2K_{g(II)}$  was not applied in data analysis

Table 2 Experimental values of pre-exponential constants, nucleation exponents, and  $\sigma\sigma_e$  for polyethylene fractions<sup>a</sup>

Assumed $T_m^\circ(\infty)$	Regime I			Regime II		
	$C_I$ ( $\text{cm s}^{-1}$ )	$K_{g(I)}$ $\times 10^{-5}$ ( $\text{K}^2$ )	$\sigma\sigma_e$ ( $\text{erg}^2 \text{ cm}^{-4}$ )	$C_{II}$ ( $\text{cm s}^{-1}$ )	$K_{g(II)}$ $\times 10^{-5}$ ( $\text{K}^2$ )	$\sigma\sigma_e$ ( $\text{erg}^2 \text{ cm}^{-4}$ )
146.5	$8.27 \times 10^{15}$	2.254	1254	$1.05 \times 10^8$	1.066	1186
145.0	$2.73 \times 10^{14}$	1.857	1037	$3.34 \times 10^7$	0.900	1008
144.0	$2.86 \times 10^{13}$	1.614	903	$1.56 \times 10^7$	0.801	897
143.0	$3.07 \times 10^{12}$	1.389	779	$7.32 \times 10^6$	0.706	793
142.5	$1.01 \times 10^{12}$	1.282	720	$5.03 \times 10^6$	0.661	743
142.0	$3.23 \times 10^{11}$	1.180	664	$3.46 \times 10^6$	0.618	695
141.5	$1.10 \times 10^{11}$	1.082	609	$2.39 \times 10^6$	0.576	648

<sup>a</sup> Values given for each assumed  $T_m^\circ(\infty)$  are the average for all nine specimens listed in Table 1



Table 3 Values of  $f, p_i$  and  $(2f/p_i)^{1/2}$  used in calculations

Assumed $T_m^\circ(\infty)$ (°C)	$\sigma$ from $\sigma\sigma_e$ with $\sigma_e = 90 \text{ erg cm}^{-2}$ <sup>a</sup>	$p_i$ at $T = 400\text{K}$	$\Delta T_t$ (°C)	$f$ at $\Delta T_t$	$(2f/p_i)^{1/2}$
146.5	13.6	3.87	17.5	0.391	0.450
145.0	11.4	4.59	16.0	0.428	0.432
144.0	10.0	5.26	15.0	0.458	0.417
143.0	8.73	6.03	14.0	0.484	0.402
142.5	8.13	6.47	13.5	0.506	0.395
142.0	7.55	6.97	13.0	0.525	0.388
141.5	6.98	7.54	12.5	0.546	0.381

<sup>a</sup> The value of  $\sigma\sigma_e$  used in this calculation is the average of the values for régimes I and II given in Table 2

should be equal. As may be seen in Table 2, these predictions hold with fair accuracy in a manner that is independent of the assumed value of  $T_m^\circ(\infty)$ .

#### Analysis of data to obtain $\sigma, p_i, n_s, L, \kappa, g_{nuc}, g_{expt}$

Once a value of  $T_m^\circ(\infty)$  and the  $P_0$  are assumed, a clear path exists that uniquely determines  $\sigma, p_i, n_s, L, \kappa$  and  $g_{nuc}$ . The procedure is as follows.

A value of  $T_m^\circ(\infty)$  is selected and the value of  $\sigma$  calculated from the corresponding estimate of  $\sigma\sigma_e$  using the value<sup>1</sup>  $\sigma_e = 90 \text{ erg cm}^{-2}$ . (This estimate of  $\sigma_e$  is that which is consistent with thermodynamic determinations of this quantity from  $T_m$  versus  $1/l$  plots.) The average of the experimental values of  $\sigma\sigma_e$  for régimes I and II is used. With  $\sigma$  known (see Table 3) one then calculates  $p_i = kT/2b_0l_u\sigma$  with  $l_u = 1.27 \times 10^{-8} \text{ cm}$ . At the same time  $f = a_0(\Delta f)/\sigma$  at  $T_t$  is found using  $a_0 = 4.55 \times 10^{-8} \text{ cm}$ . Alternatively, we can estimate the numerical factor  $(2f/p_i)^{1/2} = 2[a_0b_0(\Delta f)l_u kT]^{1/2}$  as given by equation (33). Values of  $\sigma, f, p_i$ , and  $(2f/p_i)^{1/2}$  are given in Table 3. Then using the experimentally-determined values of  $C_I$  and  $C_{II}$  for the relevant  $T_m^\circ(\infty)$  from Table 2 to calculate the ratio  $C_I/C_{II}$  for a selected value of  $P_0$ , we can find  $n_s$  using equation (32) with  $\bar{z} = 150$ , corresponding to a lamella 190 Å thick ( $10 \text{ Å} = 1 \text{ nm}$ ), and a work of chain-folding of 4900 cal mol<sup>-1</sup>, which corresponds closely to  $\sigma_e = 90 \text{ erg cm}^{-2}$  as calculated from  $q = 2a_0b_0\sigma_e$ . All our calculations with equation (32) use the coordination number  $C_n = 4$ , and  $P_0 = 1$  or  $P_0 = 25$ . The quantity  $L$  is calculated as  $n_s a_0$ . The value of  $\kappa$  is found from either equation (20) for  $C_I$  or equation (28) for  $C_{II}$  by substituting the known value of  $C_I$  or  $C_{II}$  and  $p_i, \bar{z}, n_s$ , and  $C_n P_0$ . The value of  $g_{nuc}$  is calculated according to equation (25) using the now known value of  $\kappa$ . The quantity  $g_{expt}$  is calculated from equation (5b) using the value of  $L$  derived from the above-mentioned estimate of  $n_s$ . Finally,  $g_1$  and  $g_2$  are found from equations (39) and (43) using the known values of  $\zeta_0$  (of  $D_0$ ).

## RESULTS AND CRITERIA FOR SELECTION OF BEST VALUES

The results of the calculations outlined in the preceding section are given in Table 4. The values given for  $g_{nuc}, g_{expt}, g_1$  and  $g_2$  all refer to a temperature corresponding to the régime transition, which is in general within a few degrees of 400K.

The strong dependence of  $n_s$  and  $L, \kappa$ , and  $g_{nuc}$  and  $g_{expt}$  on the assumed value of  $T_m^\circ(\infty)$  is readily discerned in Table 4. There is also some dependence of the results on the choice of  $P_0$ . We must now indicate the criteria that may be reasonably applied to these results so that best

values of the parameters may be chosen. The following criteria and restrictions, which do not *ab initio* assume any agreement between  $g_{nuc}, g_1, g_2$ , and  $g_{expt}$ , may be employed:

(1) The value of  $\kappa$  should be within an order of magnitude of unity, with values of about 5 to 10 being preferred. (See discussion in Theory section, Development of nucleation theory formulae... - above).

(2) The predicted value of the substrate length  $L$  should not much exceed  $\sim 0.5 \mu\text{m}$  ( $5000 \text{ Å}$ ). This corresponds to an upper bound for  $n_s$  of approximately  $1.1 \times 10^3$ .

The latter criterion is based on the work of Bassett *et al.*<sup>22</sup>, who found that the total lamellar width in polyethylene in the temperature range of interest here was of the order of  $1 \mu\text{m}$ . Allowing for the fact that the growth front probably has at least two faces (Figure 4), the criterion, which gives an approximate upper bound, is seen to be reasonable. The growth front may be microfaceted as illustrated schematically in Figure 4, which means that  $L$  may be considerably smaller than this approximate upper bound. It is difficult to estimate the lower bound for  $L$ , and we have arbitrarily rejected any predicted values of  $L$  that fall below  $0.05 \mu\text{m}$  ( $500 \text{ Å}$ ).

Application of the foregoing criteria to the results given in Table 4 is straightforward. The surviving results for the case  $P_0 = 1$  and  $P_0 = 25$  are marked with an asterisk (\*) in each case in Table 4. In the case  $P_0 = 1$ , only the results associated with  $T_m^\circ(\infty)$  values near  $142.5^\circ$  to  $143^\circ\text{C}$  need be considered, and in the case of  $P_0 = 25$ , only the results associated with  $T_m^\circ(\infty)$  results near  $144^\circ$  to  $145^\circ\text{C}$  require consideration. We note that  $P_0 = 25$  results are consistent in the main with the estimate of Flory and Vrij<sup>18</sup> that  $T_m^\circ(\infty) = 145.5 \pm 1^\circ\text{C}$ , while the  $P_0 = 1$  results are more nearly in accord with the contention of Wunderlich and Czornyj<sup>19</sup> that  $T_m^\circ(\infty)$  is close to the melting point of high-pressure crystallized polyethylene, which they quote as  $141.6^\circ\text{C}$ . In certain earlier work<sup>23</sup> we also utilized essentially both sets of melting points. However, it will shortly be shown that the basic issues involved in the present application of reptation to the crystallization problem can be resolved to a considerable extent without making a definitive choice for  $T_m^\circ(\infty)$  insofar as the true value is between about  $142^\circ$  and  $145^\circ\text{C}$ .

## DISCUSSION OF RESULTS

### Comparison of $g_{nuc}, g_{expt}, g_1$ and $g_2$

Consider first the results in Table 4 for  $T_m^\circ(\infty) = 142.5^\circ$  and  $143^\circ\text{C}$  for the case  $P_0 = 1$  that have met criteria (1) and (2) of the previous section. It is seen that  $g_{nuc}, g_{expt}$ , and  $g_1$

Table 4 Results of analysis of growth rate data on polyethylene fractions: estimates of substrate completion rate by various methods<sup>a</sup>

Assumed $T_m^\circ(\infty)$ (°C)	Nucleation theory, case $P_0 = 1$					Nucleation theory, case $P_0 = 25$					g by friction coefficient methods	
	$n_s$ from equation (32)	L (Å)	$\kappa$	g <sub>expt</sub> from equation (5b) and L from nucleation analysis (cm s <sup>-1</sup> )		$n_s$ from equation (32)	L (Å)	$\kappa$	g <sub>expt</sub> from equation (5b) and L from nucleation analysis (cm s <sup>-1</sup> )		g <sub>1</sub> from equation (39) (cm s <sup>-1</sup> )	g <sub>2</sub> from equation (43) (cm s <sup>-1</sup> )
				g <sub>nuc</sub> from equation (25) (cm s <sup>-1</sup> )	r <sub>s</sub> from equation (32)				g <sub>nuc</sub> from equation (25) (cm s <sup>-1</sup> )	r <sub>s</sub> from equation (32)		
146.5	$6.6 \times 10^4$	$30 \times 10^4$	155	120/n	$1.33 \times 10^4$	$6 \times 10^4$	30.8	24/n	1.43/n	0.67/n	0.43/n	
145.0	$6.60 \times 10^3$	$3.0 \times 10^4$	43.2	12/n	$1.32 \times 10^3$	$6.0 \times 10^3$	8.64*	2.4/n*	0.44/n*	0.76/n	0.43/n	
144.0	$1.43 \times 10^3$	$6.5 \times 10^3$	18.3	2.5/n	$2.85 \times 10^2$	$1.3 \times 10^3$	3.66*	0.51/n*	0.12/n*	0.82/n	0.43/n	
143.0	315*	$1.44 \times 10^3$	7.75*	0.55/n*	63	287	1.55	0.11/n	0.09/n	0.87/n	0.43/n	
142.5	148*	670*	5.05*	0.27/n*	30	134	1.00	0.05/n	0.06/n	0.90/n	0.43/n	
142.0	80	362	2.88	0.16/n	—	—	—	—	—	0.93/n	0.43/n	
141.5	33	150	2.12	0.06/n	—	—	—	—	—	0.97/n	0.43/n	

<sup>a</sup> Summary of input data:  $\sigma_e = 90$  erg cm<sup>-2</sup>,  $a_0 = 4.55 \times 10^{-8}$  cm,  $b_0 = 4.15 \times 10^{-8}$  cm,  $q = 4900$  cal mol<sup>-1</sup>,  $l_u = 1.27 \times 10^{-8}$  cm,  $\Delta h_f = 2.8 \times 10^9$  erg cm<sup>-1</sup>,  $z = 150$ ,  $\xi_0 = 3.56 \times 10^{-10}$  erg s cm<sup>-2</sup>,  $Q_D^* = 7000$  cal mol<sup>-1</sup>,  $r_f = 10^{-7}$  cm,  $C_n = 4$ . Note:  $P_0$  is the configurational path degeneracy (CPD) defined in equation (17). Asterisks (\*) denote most reasonable choices for case  $P_0 = 1$  and  $P_0 = 25$  using criteria given in text. All calculations refer to a temperature corresponding to  $\Delta T_r$ , which is within a few degrees of  $T = 400$ K

and  $g_2$  from the friction coefficient calculations, are all comparable, clearly implying that the reptation process in the melt is rapid enough at  $T \approx 400$ K to supply the substrate with molecules that undergo a considerable amount of adjacent re-entry or 'tight' folding during substrate completion. Recall that  $g_1$  and  $g_2$  begin with a direct computation of the reptation rate  $r$  from the force of crystallization and the friction coefficient for reptation in the melt, which is converted to  $g_1$  and  $g_2$  through the relation  $g = (a_0/l_g^*)r$ , which assumes adjacent re-entry. Thus, the near coincidence of  $g_1$  and  $g_2$  with  $g_{nuc}$ , the latter representing a direct computation of the substrate completion rate consistent with observed crystallization rates, strongly implies that reptation is fast enough to permit considerable adjacent re-entry or 'tight' folding.

The case  $P_0 = 25$  in Table 4, where the criteria noted in the previous section lead to consideration of the data for  $T_m^\circ(\infty)$  values in the range 144° to about 145°C, is of special interest. The quantity  $g_{nuc}$  is always either comparable to or less than the friction coefficient calculations of  $g_1$  and  $g_2$  from  $r_1$  and  $r_2$  that assume adjacent re-entry. Here one apparently has a good case for the reptation rate in the melt being rapid enough to sustain an almost total adjacent re-entry or 'tight' folding during substrate completion. However, the estimate of  $g_{expt}$  is larger than either  $g_1$  or  $g_2$ , or  $g_{nuc}$ , because  $L$  is near its upper bound. In this case it is undoubtedly wiser to draw the more conservative but still important conclusion that reptation in the melt is rapid enough to allow only part of the pendant chain—perhaps one-third to one-sixth—to enter the substrate with adjacent re-entry before an interruption occurs. This still allows a substantial amount of adjacent re-entry or tight folding, but clearly implies some interruptions in the regular folding mechanism. We regard this as the most probable interpretation, partly because it is reasonable to suppose that  $P_0 > 1$ , and partly because it implies interruptions to the regular folding process, which in turn implies the presence of an amorphous component. The resultant molecular conformation consistent with this situation is of the 'variable cluster' or 'central core' type<sup>6,24,25</sup>.

From the foregoing, one can draw the overall conclusion that the reptation process in the melt is rapid enough to permit a substantial amount of regular folding during the crystallization process in polyethylene in the temperature range considered, independent of questions concerning either  $T_m^\circ(\infty)$  or  $P_0$ .

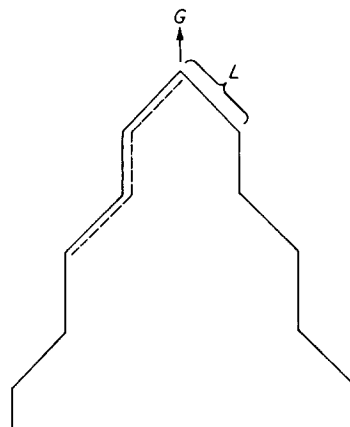


Figure 4 Microfaceted growth front (schematic). The growth front of length  $L$  is smooth in régime I, but rough in régime II owing to multiple nucleation. See text for discussion

It must be emphasized that the approximate agreement between the various estimates for  $g$  given in Table 4 does not prove that strictly adjacent re-entry occurs in crystallization from the melt, but rather that the reptation process in the melt is sufficiently rapid to permit a considerable amount of such re-entry. From both the analysis of neutron scattering experiments on highly quenched samples<sup>6,24,25</sup> and theoretical 'Gambler's Ruin' topological calculations<sup>3</sup> of the maximum number of non-adjacent events (strictly speaking non-adjacent events that lead to loops with amorphous character) that can occur, we know that the probability of regular or tight folding is equal to or greater than about two-thirds<sup>3,4,6</sup>. (This result holds for chains that are perpendicular to the plane of the chain-folds. The probability of adjacent re-entry is reduced if the chains are tilted with respect to this plane.)<sup>3</sup> A fully random re-entry or 'switchboard' model is of course impossible on topological grounds<sup>3</sup> that arise from the surface density paradox characteristic of such a construct. This difficulty is eliminated in lamellar systems by the introduction of a sufficient fraction of 'tight' folds<sup>3,6,24</sup>. Most of the tight folds are of the adjacent re-entry type. With this taken into consideration, we gain a consistent picture wherein the process in which a pendant molecule or substantial fraction thereof is reeled onto the substrate with adjacent re-entry (or very close by with no liquid-like loop) is the most probable event in the substrate completion mechanism<sup>2-4,6,24,25</sup>. Non-adjacent events certainly occur during the substrate completion process, and lead to the amorphous component that is so commonly observed. It has been shown that the kinetic theory can directly predict the presence of an amorphous component in régime II as a result of multiple nucleation on the closely spaced niches<sup>6</sup>. (The 'Gambler's Ruin' treatment<sup>3</sup> of the problem places the fraction of non-adjacent events that form either random-coil loops or tie molecules at one-third or less for vertical chain stems.) Nevertheless, these non-adjacent re-entry events do not dominate the kinetics of the crystallization process. The 'mistakes' noted above are frequent enough to lead to an amorphous component, but not numerous enough seriously to affect the kinetics or eliminate the lamellar habit. The same basic conclusion was given before<sup>1,6</sup>, but the present treatment is more precise in a number of its details.

From a practical standpoint, the principal effect of reptation is to lower the growth rate in both régimes I and II in a manner that is approximately inversely proportional to the molecular weight at a specified undercooling. This is clearly evident in Figures 2 and 3, and Table 1. It occurs because the  $1/n$  factor in  $\beta_p$ , which arises from reptation, operates both on  $i$  and  $g$ , as may be seen in equations (14) and (25).

It may be noted that the analysis with  $P_0 = 25$ , which allows  $T_m^\circ(\infty) \cong 145^\circ\text{C}$ , is consistent with values of  $\sigma$ ,  $\sigma_e$ ,  $\sigma\sigma_e$ , and  $\alpha = \sigma/(\Delta h_f)(a_0 b_0)^{1/2}$  that are quite similar to those suggested elsewhere<sup>1</sup>. For  $P_0 = 25$  we find  $\sigma = 11.4$  erg cm<sup>-2</sup>,  $\sigma_e = 90$  erg cm<sup>-2</sup>,  $\sigma\sigma_e = 1023$  erg<sup>2</sup> cm<sup>-4</sup>, and  $\alpha = 0.094$ . (The values usually quoted<sup>1,17</sup> are  $\sigma\sigma_e \sim 1250$  erg<sup>2</sup> cm<sup>-4</sup>,  $\sigma_e \sim 90$  erg cm<sup>-2</sup>,  $\sigma \sim 14$  erg cm<sup>-2</sup>, and  $\alpha \sim 0.1$ .) The use of the assumption  $P_0 = 100$  allows  $T_m^\circ(\infty)$  values somewhat higher than  $145^\circ\text{C}$  to be accommodated, in which case  $\sigma\sigma_e$ ,  $\sigma$ , and  $\alpha$  are even closer to the values commonly employed. The use of  $P_0 \sim 1$ , with its concomitant lower  $T_m^\circ(\infty)$ , leads to a lower  $\sigma\sigma_e$ , requiring

(with  $\sigma_e \cong 90$  erg cm<sup>-2</sup>) a downward adjustment of  $\sigma$  and  $\alpha$ . Modest changes in this direction will not alter the basic conclusions drawn here or in earlier analyses<sup>1</sup>. An independent estimate<sup>26</sup> of  $\sigma \cong 12.5$  erg cm<sup>-2</sup> can be derived from the homogeneous nucleation data of Turnbull and Spaepen<sup>27</sup> on the n-alkanes.

In the analysis of the data to find  $C_I$ ,  $C_{II}$ ,  $K_{g(I)}$ , and  $K_{g(II)}$  as shown in Table 2, we did not impose the condition  $K_{g(I)} = 2K_{g(II)}$ , since one of our purposes was to test this prediction of régime theory. All of the calculations given in Table 4 were based on  $C_I$  and  $C_{II}$  values taken from Table 2, i.e. they do not involve the assumption that  $K_{g(I)} = 2K_{g(II)}$ . It is of interest to note that the results are only slightly changed if the condition  $K_{g(I)} = 2K_{g(II)}$  is imposed. For example, for  $T_m^\circ(\infty) = 145^\circ\text{C}$ ,  $C_{II}$  is unchanged at  $3.34 \times 10^7$  cm s<sup>-1</sup>, and  $C_I$  is somewhat smaller at  $5.00 \times 10^{13}$  cm s<sup>-1</sup>. This gives  $L = 0.11$   $\mu\text{m}$  and  $g_{\text{expt}} = 0.44/n$  instead of  $L = 0.60$   $\mu\text{m}$  and  $g_{\text{expt}} = 2.4/n$  for  $C_n = 4$  and  $P_0 = 25$  in Table 4. The values of  $K_{g(I)}$ ,  $K_{g(II)}$ ,  $\kappa$ ,  $\sigma\sigma_e$ , and  $\sigma$  are virtually unchanged (see captions, Figures 2 and 3).

Observe that reptation is an activated process such that  $r$  and  $g$  generally become smaller with reduced temperature. Thus, at some sufficiently low crystallization temperature, reptation may become so slow as to interfere with the folding mechanism; conversely, a considerable degree of regular folding should be facilitated at higher crystallization temperatures. Some degree of regular folding could be extended to lower temperatures if the chains were tilted. In a whole polymer, where low molecular weight polymer is present in the distribution, a low molecular weight boundary layer builds up at the growth front<sup>28</sup>. This may facilitate reptation, and in turn may permit a higher degree of regular folding in whole polymers at lower crystallization temperatures than would be possible in a fraction. We note that our approach to reptation does not include the effect of 'slack' or 'stored length'. Slack could in principle facilitate the inclusion of a few stems at a time with adjacent re-entry at much lower temperatures than would be predicted with the approach given here. We note further that a considerable increase in  $g_{\text{nuc}} = g \equiv a_0(\mathbf{A} - \mathbf{B})$ , and hence the reptation velocity  $r$ , can be calculated by using  $\psi = 1/3$  rather than  $\psi = 0$  in equations (10) and (11) for  $\mathbf{A}$  and  $\mathbf{B}$ . This value of  $\psi$  is in the allowable range, and would permit folding at somewhat lower crystallization temperatures than would otherwise be the case. It is emphasized that the results given here refer to linear polyethylene. De Gennes has pointed out that large side groups and branching will affect the reptation process<sup>29</sup>. Accordingly, we would expect the reptation process, and hence the overall crystallization rate at a specified undercooling, to be slowed if such defects were present.

At a temperature well below the régime I  $\rightarrow$  régime II transition, an upward break in the growth rate will occur, which signals the onset of régime III behaviour<sup>30,31</sup> where  $G_{III} \propto i$ . This should be borne in mind in applying nucleation theory to growth rate data.

#### Comparison of nucleation theory and friction coefficient theory expressions

It is of interest to compare the various theoretical formulae that have been derived for the reptation rate associated with the crystallization process. In making these comparisons, we have used  $q = 2A_0\sigma_e$  and the

simplifications  $l_g^* \cong 2\sigma_e/(\Delta f)$  and  $\delta l \cong kT/b_0\sigma$ , and arranged the expressions so that the first bracket represents the crystalline contribution, and the second bracket the retardation factor  $\beta_g$  associated with the liquid reptation process. The symbol  $A_0$  is the cross-sectional area of the chain  $a_0b_0$ .

Consider first the reptation rate implied by equation (25), which represents the nucleation theory approach. This comes to:

$$r_{nuc} \cong a_0 \left[ \left( \frac{2\sigma_e}{\sigma} \right) \exp[-q/kT] \right] \times \left[ \left( \frac{1}{n} \right) v_0 \exp[-Q_b^*/RT] \right] \quad (45)$$

or

$$r_{nuc} \cong a_0 \left[ \frac{l_g^*}{kT} \left( \frac{\delta l}{a_0} \right) A_0(\Delta f) \exp[-q/kT] \right] \times \left[ \left( \frac{1}{n} \right) v_0 \exp[-Q_b^*/RT] \right] \quad (46)$$

where the frequency factor  $v_0$  with the value  $\kappa \cong 10$  is found to be:

$$v_0 = \kappa(kT/h) \sim 8.3 \times 10^{13} \text{ s}^{-1} \quad (47)$$

Notice that the crystalline part can be written as a numerical factor multiplied by the force  $A_0(\Delta f)$  exerted on a chain during stem formation.

From the approaches to the calculation of  $r$  involving the two expressions for the mean force of crystallization on a reptating molecule, wherein the resistance in the melt is given by the overall friction coefficient  $\zeta_0 n$ , we have first the expression where the force is proportional to the derivative of the smoothed potential with respect to substrate length:

$$r_1 = \frac{\bar{f}_{1(c)}}{\zeta_0 n} \cong a_0 \left[ \frac{\Delta f}{2\sigma_e} A_0(\Delta f) \right] \times \left[ \left( \frac{1}{n} \right) v_0 \exp[-Q_b^*/RT] \right] \quad (48)$$

where the frequency factor is:

$$v_0 = (kT/\zeta_0 A_0) \exp(Q_b^*/RT_0) \sim 5.5 \times 10^{14} \text{ s}^{-1} \quad (49)$$

at  $T_0 = 400\text{K}$ .

Meanwhile we may write the reptation rate connected with the second approximation for the mean force  $\bar{f}_{2(c)}$ , i.e. the time average force of crystallization, which comes to:

$$r_2 = \frac{\bar{f}_{2(c)}}{\zeta_0 n} = a_0 \left[ \frac{l_g^*}{kT} \left( \frac{b_0}{l_f} \right) A_0(\Delta f) \exp[-q/kT] \right] \times \left[ \left( \frac{1}{n} \right) v_0 \exp[-Q_b^*/RT] \right] \quad (50)$$

Note first that the liquid state retardation function  $\beta_g$  found using formulae based on  $r \propto \text{force/friction}$  coefficient, namely equations (48) and (50), are identical in general form to that assumed in earlier work for the nucleation process, equation (16). Comparison of equations (45) or (46) and equation (50) shows that even the numerical values of the effective frequency factors  $v_0$  and  $v_0'$  are rather similar. Note also that the  $1/n$  dependence arises in a natural way in equations (48) and (50). Accordingly, we consider the general form of  $\beta_g$  that was assumed in equation (16) to be justified for use in nucleation approach expressions such as equations (10)–(13).

Consider now the crystalline contribution to the reptation rate as it is revealed by the first bracket in the above expressions. The strongest similarity is seen to exist between  $r_{nuc}$  and  $r_2$ , both of which contain the factor  $l_g^* \exp(-q/kT) \propto \sigma_e \exp(-q/kT)$  which clearly brings out the role that chain-fold formation has in reducing the rate of reptation and therefore the rate of substrate completion by lowering the effective force of crystallization. These expressions are also similar in that both  $r_2$  and  $r_{nuc}$  explicitly contain a force as evidenced by the factor  $A_0(\Delta f)$ . As can be seen from Table 4, there is little to choose between  $g_{nuc}$  and  $g_2$ , and hence  $r_{nuc}$  and  $r_2$ , as regards their absolute numerical values in the temperature range of interest here (see data in Table 4). Observe also that the dependences on temperature of the crystalline contribution of  $r_{nuc}$  and  $r_2$  are, apart from a trivial factor of  $1/T$ , quite similar.

The expression for the crystalline part of  $r_1$  stands out as being rather different from both  $r_{nuc}$  and  $r_2$ , though it is clear from Table 4 that the corresponding  $g_1$ ,  $g_2$ , and  $g_{nuc}$  values, and hence the absolute magnitude of  $r_1$ ,  $r_2$ , and  $r_{nuc}$ , are similar. In  $r_1$ , the work of chain-folding appears as  $q^{-1}$ , whereas in  $r_{nuc}$  it is of the form  $q \exp(-q/kT)$ . While the  $q^{-1}$  dependence is in the right direction in that it suppresses the reptation rate with increasing work of chain-folding, it seems probable to us that the form of  $r_{nuc}$  and  $r_2$  is more nearly correct in this respect. Note also that  $r_1$  varies as  $(\Delta T)^2$ , while  $r_{nuc}$  and  $r_2$  do not depend on the undercooling.

On balance, we consider the form of  $r_{nuc}$  and  $r_2$  to be more revealing as regards the factors that actually control the reptation rate that occurs during the crystallization process.

It is useful to give a further generalization of the results. It is seen from the foregoing that the liquid retardation factor that we have generally denoted  $\beta_g$  when derived from the expression  $r = \bar{f}_c/\zeta_0 n$  is always given by  $\beta_g = (1/n)v_0' \exp(Q_b^*/RT)$  where  $v_0'$  is as quoted in equation (49). Recall that this is of exactly the form assumed in earlier work (see equation (16)).

If we now insert a factor  $\kappa'$  that is the order of unity in this expression to allow for minor adjustments consistent with experiment to obtain:

$$\beta_g = (\kappa'/n)v_0' \exp(-Q_b^*/RT) \quad (51)$$

where  $v_0'$  is  $(kT/\zeta_0 A_0) \exp(Q_b^*/RT_0)$  as before, where  $T_0 = 400\text{K}$  is the reference temperature, we can use this  $\beta_g'$  in the fundamental nucleation rate expressions given by equations (10)–(13) in place of equation (16) to find a self-consistent combined nucleation–reptation theory approach that yields:

$$g = a_0(\mathbf{A} - \mathbf{B}) = a_0 \left[ \frac{a_0}{kT} \left( \frac{\delta l}{a_0} \right) A_0(\Delta f) \exp(-q/kT) \right] \times \left[ \left( \frac{\kappa'}{n} \right) v'_0 \exp(-Q_b^*/RT) \right] \quad (52)$$

and:

$$r = a_0 \left[ \frac{l_g^*}{kT} \left( \frac{\delta l}{a_0} \right) A_0(\Delta f) \exp(-q/kT) \right] \times \left[ \left( \frac{\kappa'}{n} \right) v'_0 \exp(-Q_b^*/RT) \right] \quad (53)$$

The foregoing in effect conjoins the two apparently different theoretical approaches to the reptation rate and substrate completion rate problems set forth in this paper.

It may be noted that our result for the behaviour of a reptating segment emerges as a product of a friction coefficient or 'viscosity' term and an activation energy term (see equation (51)). This is precisely the same form that is found in an elegant treatment of a particle in a double well in a highly viscous medium in the so-called high coupling limit<sup>32,33</sup>.

A consideration of the  $g_{nuc}$  and  $g_{expt}$  data marked (\*) in Table 4 and the corresponding  $g_1$  and  $g_2$  values, together with the expressions given in this section, leads to the definite impression that the substrate completion process is jointly governed by reptation in the melt and the necessity of forming a chain-fold for the majority of stems that are laid down.

#### The Lauritzen Z test: alternative calculation of $n_s$ and L

The transition between régime I and régime II can be predicted by consideration of the dimensionless parameter<sup>1,7</sup>:

$$Z = iL^2/4g = in_s^2 a_0^2/4g \quad (54)$$

If Z is  $\sim 0.1$  or less, crystallization is in régime I, and if Z is unity or greater, crystallization is in régime II. Using equations (18) and (25) for  $i$  and  $g$ , and substituting numerical values for  $\bar{z}$ ,  $q$ , and the other quantities we find:

$$n_s^2 = Z_{crit}(\Delta T_i) \times 1.63 \times 10^{-7} \exp[K_{g(1)}/T(\Delta T_i)] \quad (55)$$

for  $P_0=1$  and  $C_n=4$ . Taking the value of Z at the transition to be  $Z_{crit}=0.5$  it is a simple matter to estimate  $n_s$  if the  $\Delta T_i$  of the transition is known. For example, if we take  $\Delta T_i=13.5^\circ\text{C}$  for  $T_m^\circ(\infty)=142.5^\circ\text{C}$  from Table 4, and  $K_{g(1)}=1.282 \times 10^5$  from Table 2, it is readily verified that the above expression yields  $n_s \cong 141$ , giving an L of 643 Å which is in good agreement with the value of 670 Å calculated from equation (32) given in Table 4 for  $P_0=1$ . Similar agreement is obtained for the case  $P_0=25$ ,  $C_n=4$  for  $T_m^\circ(\infty)=145^\circ\text{C}$ .

#### Morphological implications

The analysis given in Table 4 does not uniquely imply that the effective substrate length L is substantially less than about one-half of the lamellar width, even though much of the data are consistent with this concept. The possible exception is the  $L=6000$  Å value for

$T_m^\circ(\infty)=145^\circ\text{C}$  for the case  $P_0=25$ . Here the predicted value of L is comparable to about one-half the lamellar width, which implies that microfaceting may not be present. Nevertheless, one must consider the possibility that the growth front is microfaceted in régime I as illustrated schematically in Figure 4. There is also the possibility that L is more accurately represented as a 'persistence length'<sup>1</sup> on a somewhat crenelated growth front rather than as an actual microfacet as shown in Figure 4. L may be a function of growth temperature, but such a variation would not alter our basic conclusions.

If the growth front is microfaceted, we might expect two or more types of folds to occur in melt-crystallized polyethylene: one type of fold (which we have assumed here to be [110]) would correspond to L, while those that occur more nearly parallel to the direction of growth might correspond for instance to [200] or [310], or some other plane. Neutron scattering studies on melt-crystallized PE suggest the existence of other than [110] type folds in melt-crystallized polyethylene<sup>24,25</sup> and infrared studies on single crystals imply the presence of both [110] and [200] fold planes<sup>34</sup>.

In régime II the substrate of length L will suffer multiple nucleation and therefore be quite rough.

#### Molecular weight dependence of absolute growth rate: reptation times

An analysis of the growth rate data of the type depicted in Figure 3 at a fixed undercooling near the centre of régimes I and II shows that for all nine specimens studied,  $G \propto 1/n_z^{1.3 \pm 0.3}$ . This holds for both régimes. The error quoted is the standard deviation. A further analysis shows that a somewhat weaker dependence with a larger standard deviation than this is found if  $n_w = M_w/14.0$  is used. An analysis where  $n = n_n = M_n/14.0$  is employed fails to reveal any clear dependence of G on n. Thus the predicted  $1/n$  behaviour of G refers to a molecular weight average that is near, but probably slightly below,  $M_z$ . It is not surprising that the longer molecules in the distribution tend to control the reptation process involved in substrate completion.

It has been shown elsewhere that the time required for reptation  $t_r$  is given by<sup>10</sup>:

$$t_r = \frac{1}{2} \left( \frac{\mathcal{L}}{r} \right) = \frac{1.27 \times 10^{-8} n_z}{2r} \quad (56)$$

Notice that since the reptation rate  $r$  varies as  $1/n_z$ , the reptation time actually varies as  $n_z^2$ . Using  $g_{nuc} \cong 0.5/n$  from Table 4 to get  $r_{nuc} = 21/n$ , one finds that  $t_r = 9.8 \times 10^{-4}$  s for the lowest molecular weight studied ( $n_z = 1800$ ) and  $6.4 \times 10^{-2}$  s for the highest ( $n_z = 14540$ ). For  $n_z = 7143$ , which corresponds to  $M_z = 10^5$ , one gets  $t_r = 1.5 \times 10^{-2}$  s as compared with  $1.0 \times 10^{-2}$  s from a previous treatment<sup>10</sup>.

The above calculations imply that the shorter molecules in the distribution would tend to enter the substrate at a more rapid rate than the longer ones. This holds only for pendant chains of moderate to high molecular weight, provided of course that multiple nucleation of the chain has not occurred. On the other hand, very short molecules (say only several times  $l_g^*$  in length) will experience a considerably lower driving force and tend to be rejected during the nucleation and substrate completion processes.

*Entanglements in melt*

If the traditional views of melt shear viscosity applied to the rate at which molecules could be supplied to the growth front, one would expect the growth rate at a fixed undercooling to vary as  $\sim M^{-3.4}$  above the so-called 'entanglement point', which is at  $M_w \sim 3830$  or  $n \sim 273$  for polyethylene<sup>35</sup>, and as  $\sim M^{-1}$  below this point. No such behaviour is found at high molecular weights: instead, the growth rate varies in the range  $n_z = 1900$  to  $n_z = 14500$  approximately as  $M_z^{-1}$ . This clearly means that the 'entanglements' that are said to cause the molecular weight dependence of the viscosity to change from  $\sim M^1$  to  $M^{3.4}$  near  $M = 3830$  are not operative as retardations to molecules entering the growth front in the crystallization process even at the higher molecular weights treated here. The resolution of this apparent discrepancy is of course that the steady-state reptation process is not seriously affected by the temporal entanglements that alter viscous flow above  $M = 3830$ . The steady-state reptation process in the long time scale involved in Regimes I and II in effect avoids the effect of entanglements.

That entanglements play no role in determining the molecular weight dependence of the customary centre-of-mass diffusion coefficient  $D_{CM}$  in polyethylene has already been shown by Klein and Briscoe<sup>14</sup>. Up to  $M = 23000$ , they demonstrated that  $D_{CM}$  varies as  $M^{-2.0}$ , which is precisely what the reptation model of diffusion predicts. (It may be recalled that if  $D_{CM} = D_0 M^{-2}$ , the reptation model where the friction coefficient is proportional to the length of the molecule as  $\zeta = \zeta_0 n$  is clearly indicated<sup>36,37</sup>.) The present work implies that the law  $D_{CM} = D_0 M^{-2}$  also applies at least approximately at considerably higher molecular weights than were investigated by Klein and Briscoe.

*Activation energy of reptation in melt and undercooled state*

Klein and Briscoe<sup>14</sup> have shown by experiment that the activation energy for reptation in a polyethylene melt is  $Q_D^* = 7000 \text{ cal mol}^{-1}$ . This determination centred around a temperature of 449K, which is well above the melting point. In the present work we have used this same value of  $Q_D^*$  to represent the activation energy for the reptation transport process in the subcooled state centring about the reference temperature of  $T_0 = 400\text{K}$ . It is doubtful if this leads to any significant error in the analysis, but an intriguing question arises in connection with the temperature dependence of the activation energy of the liquid transport process as it affects polymer crystal growth at low crystallization temperatures.

Some time ago it was suggested<sup>23</sup> that at temperatures below the maximum in the growth rate the transport process that governed the rate there was of the general form  $\exp[-U^*/R(T - T_\infty)]$ . Originally the so-called Williams-Landel-Ferry<sup>35</sup> constants  $U^* = 4120 \text{ cal mol}^{-1}$  and  $T_\infty = T_g - 51.6^\circ\text{C}$  derived from viscosity measurements were suggested; but Kovacs and Suzuki<sup>38</sup> found  $U^* \cong 1500 \text{ cal mol}^{-1}$  and  $T_\infty = T_g - 30^\circ\text{C}$  for isotactic-polystyrene by crystallization rate measurements, and similar values were found for some other polymers<sup>1</sup>. In brief, the activation energy that controls the liquid transport process impeding crystallization is at low temperatures temperature dependent, and acts as if it is approaching infinity at the finite temperature  $T$ . The transport factor  $\exp[-U^*/R(T - T_\infty)]$  with values of  $U^*$

and  $T_\infty$  adjusted somewhat to approximate the effect of  $\exp(-Q_D^*/RT) = \exp(7000/RT)$  at high temperatures could have been used in the present analysis with no difficulty or change in interpretation. In fact, it is generally preferable to use  $\exp[-U^*/R(T - T_\infty)]$  in the analysis of growth rate data, especially in the case where data below the maximum in the growth rate are to be dealt with<sup>1</sup>. This was not necessary in the present case of polyethylene fractions—first, because an independently determined value of  $Q_D^*$  was available, and secondly, because the growth rate data were in a temperature region far above the maximum in  $G$ , where the temperature dependence of  $-U^*/R(T - T_\infty)$  is minimal.

It is of interest to pose the question of whether the semi-empirical expression  $\exp[-U^*/R(T - T_\infty)]$  implies the freezing out of reptation at  $T_\infty$ . If this provisional identification is correct, then it would appear that the reptation process associated with crystallization essentially ceases at  $T_\infty \cong T_g - 30^\circ\text{C}$ . It has recently been suggested<sup>30</sup> that the factor  $\exp[-U^*/R(T - T_\infty)]$ , when used at low temperatures in Regime III, refers to retardations associated with 'slack' portions of the pendant chains. The factor  $\exp[-Q_D^*/RT]$  used for analysis in the body of this paper refers to the steady-state reptation process, where the friction coefficient is proportional to the length of the pendant chain.

## CONCLUSIONS

(1) Nucleation theory has been adapted to include the concept of reptation by introducing a factor of  $1/n$  in the liquid state retardation parameter  $\beta_g$  that multiplies the elementary rate constants  $A_0$ ,  $B_1$ ,  $A$ , and  $B$ . This causes both the nucleation rate  $i$  and the substrate completion rate  $g$  to vary as  $1/n$ , leading the predicted growth rates in régime I ( $G_I$  varies as  $i$ ) and régime II ( $G_{II}$  varies as  $(ig)^{1/2}$ ) to fall with increasing molecular weight. This is confirmed by experiment in the case of polyethylene fractions.

(2) Explicit expressions are derived from nucleation theory for  $g$  and the corresponding reptation rate  $r$ . Numerical values are estimated for these quantities that are consistent with the growth rate data on the fractions.

(3) An alternative theory, which calculates the reptation rate as  $r = (\text{force of crystallization}) \div (\text{friction coefficient for reptation in melt})$  is set forth. When  $r$  is converted to  $g$  using the assumption of adjacent re-entry chain-folding, this approach gives numerical results for  $g$  for polyethylene fractions in the temperature range of interest that are quite similar to those estimated from nucleation theory.

(4) It is shown how the substrate completion rate can be found directly from growth rate data and an estimate of the substrate length  $L$ . Here there is no assumption concerning adjacent re-entry. The numerical values of  $g_{\text{expt}}$  found in this way are roughly comparable to those calculated from the nucleation theory and the friction coefficient theory approaches using the assumption of regular folding.

(5) The conclusion is drawn that the rate of reptation in the melt is sufficiently rapid to permit a significant fraction of each pendant molecule to enter the substrate with regular folding. Thus, it does not appear that retardations in the melt are sufficiently large to prevent considerable adjacent re-entry or 'tight' folding under the conditions

stated. Reptation clearly provides a plausible mechanism whereby the force of crystallization can extract a polymer molecule, or a significant part of it, from the inter-entangled melt. Within reasonable limits, the foregoing conclusion is independent of the melting point that is assumed for polyethylene in the analysis.

(6) The reptation rate calculated from nucleation theory and the preferred form of the friction coefficient theory can each be cast in the form:

$$r = (\text{Constant}) \times (A_0 \cdot \Delta f) \exp(-q/kT) \times (1/m) \exp(-Q_b^*/RT)$$

where  $A_0 \cdot \Delta f$  = force of crystallization,  $q$  = work of chain folding,  $n$  = number of chain units in pendant molecule, and  $Q_b^*$  = activation energy for reptation in melt. To a good approximation,  $q$  can be calculated from  $r$  as  $r(a_0/l_q^*)$ . The friction coefficient approach gives a liquid retardation parameter  $\beta_g$  of the form  $(1/n)v_0' \times \exp(-Q_b^*/RT)$ , which is similar to that proposed earlier for the nucleation approach.

(7) The data analysis on the polyethylene fractions show that the predictions of régime theory, particularly the change of slope of the growth rate at the transition, are closely obeyed. Also, the treatment is consistent with the Lauritzen  $Z$  test. Again, these conclusions are independent of the melting point assumed for polyethylene.

(8) The theory given allows the possibility that the growth tip may be microfaceted, but the data do not uniquely demand this result. In general, the growth rate data are consistent with a substrate length  $L$  that is within a factor of about five of  $0.1 \mu\text{m}$ .

(9) The treatment is consistent with the presence of some non-adjacent re-entry events, i.e. loops or interlamellar links, during substrate completion, which in turn is consistent with the existence of an amorphous component. From independent studies, it is known that about two-thirds of the stems enter the substrate with tight folding, much of this with adjacent re-entry. Therefore, the assumption of regular folding used in the elementary treatment should be a relatively good one with respect to prediction of kinetic behaviour, and this is supported by the analysis of the rate data. Some of the rate data imply the presence of occasional interruptions to regular folding during substrate completion. The interruptions caused by non-adjacent re-entry do not in any event seriously alter the kinetics or eliminate the lamellar habit.

(10) The numerical values of  $\sigma\sigma_e$ ,  $\sigma$ ,  $\sigma_e$ , and  $\alpha$  obtained from the present treatment are quite similar to those found in previous studies, especially in the case where  $T_m^{\infty} \cong 145^\circ\text{C}$ . The present treatment allows a range of  $T_m^{\infty}$  values to be used in the analysis without any basic change in physical interpretation.

#### ACKNOWLEDGEMENT

The author is grateful to Drs C. M. Guttman, E. A. DiMarzio, E. Passaglia, G. T. Davis, F. Khoury and L. Frolen of the National Bureau of Standards, Dr A. J. Kovacs, Centre De Recherches sur les Macromolécules, Strasbourg, France, for many helpful discussions and for much useful criticism.

#### REFERENCES

- Hoffman, J. D., Davis, G. T. and Lauritzen Jr, J. I. in 'Treatise on Solid State Chemistry' (Ed. N. B. Hannay), Plenum Press, New York, 1976, Vol. 3, Ch. 7
- Khoury, F. and Passaglia, E. in 'Treatise on Solid State Chemistry' (Ed. N. B. Hannay), Plenum Press, New York, 1976, Vol. 3, Ch. 6
- Guttman, C. M., DiMarzio, E. A. and Hoffman, J. D. *Polymer* 1981, **22**, 1466
- DiMarzio, E. A. and Guttman, C. M. *Polymer* 1980, **21**, 733
- DiMarzio, E. A., Guttman, C. M. and Hoffman, J. D. *Discuss. Faraday Soc.* 1979, **68**, 210
- Hoffman, J. D., Guttman, C. M. and DiMarzio, E. A. *Discuss. Faraday Soc.* 1979, **68**, 177
- Lauritzen Jr, J. I. *J. Appl. Phys.* 1973, **44**, 4353
- Frank, F. C. *J. Crystal Growth* 1974, **18**, 111
- Lauritzen Jr, J. I. and Hoffman, J. D. *J. Appl. Phys.* 1973, **44**, 4340
- Hoffman, J. D. *Discuss. Faraday Soc.* 1979, **68**, see discussion remarks pp. 386
- Lauritzen Jr, J. I. and Passaglia, E. *J. Res. Nat. Bur. Stand. (A)* 1967, **71**, 261
- Point, J. *J. Discuss. Faraday Soc.* 1979, **68**, 167
- Classical nucleation theory assigns a probability to each possible crystallization path, and then calculates the total flux by summing over all such paths: thus  $S_T = \sum S_i$ . Because of the extreme mathematical complexity of considering a large set of paths, we must in practice select a small set that is representative of the most probable paths. If we call  $S$  the most probable path, then
 
$$S_T = \sum_i S_i = P_0 S$$
 defines a configurational path degeneracy  $P_0$ . This is explicitly brought out, for instance, in the LP treatment [ref 11]. The fact that values of  $P_0$  in the range of 1 to 25 (and even upwards of 100) give a reasonable fit of the data, with some preference for cases where  $P_0 > 1$ , suggests that the proposed revision of the kinetic theory, though simple, contains most of the relevant physics
- Klein, J. and Bischof, B. *J. Proc. Roy. Soc. London (A)* 1979, **365**, 53
- Jones, D. H., Latham, A. J., Keller, A. and Girolamo, M. *J. Polym. Sci., Polym. Phys. Edn.* 1973, **11**, 1759
- Barham, P. J., Chivers, R. A., Jarvis, D. A., Martinez-Salazar, J. and Keller, A. *Polym. Lett.* 1981, **19**, 539
- Hoffman, J. D., Frolen, L. J., Ross, G. S. and Lauritzen Jr, J. I. *J. Res. Nat. Bur. Stand. (A)* 1975, **79**, 671
- Flory, P. J. and Vrij, A. *J. Am. Chem. Soc.* 1963, **85**, 3548
- Wunderlich, B. and Czornyj, G. *Macromolecules* 1977, **10**, 906
- Broadhurst, M. G. *J. Chem. Phys.* 1962, **36**, 2578
- Broadhurst, M. G. *J. Res. Nat. Bur. Stand. (A)* 1966, **70**, 481
- Bassett, D. C., Hodge, A. M. and Olley, R. H. *Discuss. Faraday Soc.* 1979, **68**, 218
- Hoffman, J. D. *SPE Trans.* 1964, **4**, 315
- Guttman, C. M., Hoffman, J. D. and DiMarzio, E. A. *Discuss. Faraday Soc.* 1979, **68**, 297
- Guttman, C. M., Hoffman, J. D. and DiMarzio, E. A. *Polymer* 1981, **22**, 597
- Hoffman, J. D. *Discuss. Faraday Soc.* 1979, **68**, see discussion remarks pp. 371
- Turnbull, D. and Spaepen, F. *J. Polym. Sci., Polym. Symp.* 1977, **59**, 31
- Keith, H. D. and Padden, F. J. *J. Appl. Phys.* 1964, **35**, 1270
- De Gennes, P. G. *Discuss. Faraday Soc.* 1979, **68**. See discussion remarks pp. 381
- Hoffman, J. D. manuscript in preparation
- Hoffman, J. D. *Discuss. Faraday Soc.* 1979, **68**. See discussion remarks pp. 378
- Skinner, J. L. and Wolynes, P. G. *J. Chem. Phys.* 1978, **69**, 2143
- Kramers, H. A. *Physica (The Hague)* 1940, **7**, 284
- Krimm, S. and Cheam, T. C. *Discuss. Faraday Soc.* 1979, **68**, 244, and earlier papers referred to therein
- Ferry, J. D. 'Viscoelastic Properties of Polymers', 2nd Edn., Wiley, New York, 1970
- De Gennes, P. G. *J. Chem. Phys.* 1971, **55**, 572
- De Gennes, P. G. *Macromolecules* 1976, **9**, 591
- Suzuki, T. and Kovacs, A. J. *Polymer* 1970, **1**, 82